IEEE Access
Multidisciplinary ⋮ Rapid Review ⋮ Open Access Journal

Received 14 February 2024, accepted 1 March 2024, date of publication 4 March 2024, date of current version 4 April 2024.

Digital Object Identifier 10.1109/ACCESS.2024.3373539

RESEARCH ARTICLE

DermCDSM: Clinical Decision Support Model for Dermatosis Using Systematic Approaches of Machine Learning and Deep Learning

RUCHI MITTAL[1], FATHE JERIBI[2], R. JOHN MARTIN[2], VARUN MALIK[1], (Member, IEEE), SANTHOSH JOSEPH MENACHERY[3], AND JAITEG SINGH[1]

[1]Chitkara Institute of Engineering and Technology, Chitkara University, Rajpura, Punjab 140401, India
[2]College of Engineering and Computer Science, Jazan University, Jazan 45142, Saudi Arabia
[3]College of Pharmacy, Jazan University, Jazan 45142, Saudi Arabia

Corresponding author: Fathe Jeribi (fjeribi@jazanu.edu.sa)

The authors extend their appreciation to the Deputyship for Research & Innovation, Ministry of Education in Saudi Arabia for funding this research work through the project number ISP23-78.

ABSTRACT Skin disorders encompass a wide range of conditions that affect the skin, a vital organ of the human body. Early detection of skin diseases is difficult due to a lack of awareness, subtle symptoms, similarities, inter-individual heterogeneity in symptoms, limited access to dermatologists, and difficulties in imaging techniques. In this article, we propose a clinical decision support model for detection and classification of skin diseases (DermCDSM) through productive improvement of division capabilities and a cross-breed profound learning procedure. The division cycle is expected to be further developed using an improved chameleon swarm optimization (ICSO) method that takes into account a more accurate and proficient identification of the main cause of the disease. By employing the ICSO algorithm, we aim to enhance the overall accuracy and reliability of disease detection methods. Multi-strategy seeking optimization (MSSO), which is used to optimize feature selection by identifying the most significant features for the task at hand, has been introduced to handle the tests connected to data dimensionality. Convolutional deep spiking neural networks (CD-SNN), a deep learning method, have been implemented to improve the precision of skin cancer diagnosis and multi-class classification. The benchmark ISIC 2017 dataset is utilized to validate the efficacy of our proposed framework, DermCDSM, and its superiority over existing approaches in terms of accuracy, dependability, and efficiency is demonstrated.

INDEX TERMS Decision support system, deep learning, eczema, digital healthcare, image segmentation.

I. INTRODUCTION

Skin disease refers to any condition or disorder that affects the skin, which is the body's major organ [1]. There are numerous types of skin diseases, ranging from common conditions like acne, eczema, and psoriasis to more serious diseases such as skin cancer and infectious diseases like fungal or bacterial infections [2]. Skin diseases manifest in various ways, including rashes, itching, redness, inflammation, discoloration, and the formation of lesions or bumps on the skin. Therapy for skin conditions can vary depending on the particular condition and may involve skin prescriptions, oral medications, lifestyle changes, or surgical procedures [3]. Skin diseases can be diagnosed using a variety of methods, including visual examination by dermatologists or other healthcare professionals and clinical considerations. Dermoscopy is an imaging technique, and there have also been innovative improvements, including PC-assisted diagnostic systems [4], [5]. Recently, significant progress has been made in managing skin diseases using computerized reasoning approaches [6]. Computerized reasoning systems can discover patterns in massive datasets, learn from them, and make extremely precise predictions. This enables early detection, diagnosis, and treatment of various skin conditions [7].

Clinical decision support for skin disorders plays a crucial role in accurate diagnoses, facilitating appropriate treatment

The associate editor coordinating the review of this manuscript and approving it for publication was Yiqi Liu.

plans, and monitoring the progress of skin conditions [6], [8]. Dermatologists and healthcare professionals can visually analyze high-resolution images, identifying distinct patterns, textures, colors, and other visual characteristics associated with different skin diseases [9]. In addition to visual examination, image processing methods are successful in locating hotspots in skin images [10]. Relevant features such as shape, texture, color, and lesion size can be extracted using specialized algorithms. These extracted features act as significant discriminative factors [11] for distinguishing between different types of skin diseases. By quantifying and analyzing these features, image processing aids in the automated classification and diagnosis of skin conditions, enabling more accurate and efficient detection [12]. Another advantage of image processing in skin disease detection is its capability to preprocess and enhance the quality of skin images [13]. Often, noise, artifacts, and varying lighting conditions distort skin imagery. To address these issues, image processing algorithms can perform tasks such as noise reduction, image enhancement, and normalization [14]. By applying these preprocessing techniques, the quality of skin images is improved, ensuring more accurate and consistent analysis. Image segmentation is a critical step in skin disease detection, and image processing techniques excel in this area as well [15], [16], [17].For separating damaged skin from healthy skin, segmentation algorithms are used. Image processing techniques, in conjunction with machine learning and pattern recognition [18], also contribute to computer-aided diagnosis systems for skin diseases. These technologies can help dermatologists make decisions by offering computer-aided diagnosis [36], [37], providing another perspective, and leading to more accurate and consistent diagnoses [19]. We propose a novel technique to enhance the early detection and classification of skin diseases, by combining efficient segmentation and feature optimization with a hybrid deep learning approach. The proposed technique offers several significant contributions, which are summarized as follows:

1. An improved Chameleon Swarm Optimization (ICSO) algorithm that aims to improve the segmentation process for more efficient and precise identification of the targeted disease region. This algorithm addresses the challenges associated with data dimensionality and provides better results.
2. Introduced the Multi-Strategy Seeker Optimization (MSSO) technique to address the issue of high-dimensional data. MSSO optimizes feature selection by identifying the most relevant and informative features specifically tailored to the given task.
3. Integrated a Convolutional Deep Spiking Neural Network (CD-SNN) into our framework to enhance the accuracy of skin cancer detection and enable multi-class classification.

Overall, our proposed approach utilizes the ICSO algorithm for improved segmentation, employs the MSSO technique for feature selection, and incorporates the CD-SNN model for accurate skin cancer detection and multi-class classification. These advancements aim to enhance the efficiency, precision, and overall performance of skin disease analysis, ultimately benefiting healthcare professionals and patients in diagnosing and treating skin conditions. The structure of the remainder of this article is as follows: Section Two presents the detailed analysis of the benchmarked works for the identification of skin infections. Section Three presents the evolution of the research problem and the methodologies adopted. Section Four presents the results of the experiments and a comparative analysis of the proposed and existing techniques, and Section Five concludes.

II. RELATED WORKS

This section offers a thorough analysis of the most recent publications that are significant in identifying and classifying skin diseases. This section's goal is to lay out developments and research initiatives in this field while emphasizing the important contributions and findings of each work. We obtain useful insights into the current state-of-the-art techniques and methods utilized for skin disease detection and classification by reviewing this related literatures. Table 1 summarizes the research gaps identified in these works.

Gavrilov et al. [20] have proposed an innovative approach for automatic diagnostics of skin neoplasms by means of a convolutional deep learning neural network. Their model demonstrates more accuracy in the qualitative diagnosis of skin melanoma, achieving a minimum accuracy of 91%. Chen et al. [21] developed a real-time, flexible, and adaptable system for detecting skin diseases. The method used in this procedure requires constant data flow between the client and a clinical server, which stores a variety of information, such as images of the client's skin, the patient's overall health state, and model requirements. By selecting significant information at the edge node, the system increases model generalization and data quality in the remote cloud database. To demonstrate the adaptability of their algorithm, three learning models (LeNet-5, AlexNet, and VGG16) were trained on the cloud.

Bu et al. [22] have developed a skin disease taxonomy based on cytology and pathology and compared it to the ICD-10 system in terms of its predictive power. The taxonomy consists of six levels and organizes individual diseases in a hierarchical tree structure. The study's findings demonstrated that the developed taxonomy outperformed the ICD-10 system in predicting skin diseases.Likewise, Mijwil [23] proposed a deep learning network for the analysis of a large dataset consisting of over 24,000 skin cancer images. The results showed that the InceptionV3 architecture achieved highly satisfactory outcomes, demonstrating its ability to generalize the detection of cancer in the images. Diagnostic accuracy was 86.90%, accuracy was 87.47%, sensitivity was 86.14 percent, and specificity was 87.66% for the InceptionV3 architecture.

Khan et al. [24] proposed a fully automatic computer-aided diagnosis system for skin scratch analysis using a deep learning framework. The MASK-RCNN algorithm is then

TABLE 1. Summary of research gaps.

Ref.	Method	Classifier	Dataset	Accuracy (%)	Concerns and how they are handled by this work	Other Research gaps
[20]	Diagnostics of skin diseases	ACNN	ISIC 2017	91.0	The data imbalance problems that were not solved in [20], these issues are addressed in this work.	-
[21]	Skin disease recognition	LeNet-5, AlexNetV, GG16	Wuhan Union Hospital	89.6	In [21], the false acceptance rate was not considered, which is addressed by CD-SNN in this work.	Leading to a high error rate in traditional diagnostic approaches.
[22]	Prediction of skin disease	Deep residual learning	Atlas, Dermatoweb	91.7	The design of classifiers in [22] is very expensive, a problem that is solved in this work.	The current cost of such a specialized diagnosis remains limited and often expensive.
[23]	Skin cancer disease classification	ConvNet-Inception-V3, ResNet, VGG19	ISIC 2019 and ISIC 2020	86.9	The prediction model in [23] faces the dimensionality issue, which is addressed by MSSO.	Due to the utilization of different image datasets, the models can be conflicting and confusing.
[24]	Skin lesion detection and recognition	MASK-RCNN	ISBI2016, ISBI2017	93.6	Limited by minimum accuracy as mentioned in [24], the CD-SNN technique is utilized here to improve it.	Posing challenges in terms of scalability and feasibility.
[25]	Diagnosis of skin disease	Modified-MobileNet	DermWeb	94.8	The computational complexity of MobileNet in [25] is high, a problem that is solved by feature optimization.	Limited specifications and computational power.
[26]	Skin disease classification	TEMCM-MobileNet	HAM10000	94.3	MobileNet [26] failed to optimize features, so we use the ICSO algorithm to improve performance.	Limiting its application to more complex multi-class scenarios.
[27]	Classification of skin disease	MobileNet V2 and LSTM	HAM10000	85.0	Despite using LSTM in [27], optimization issues persist, which are resolved by the MSSO algorithm.	Data dimensionality issues can have an impact on the model's performance and accuracy.
[28]	Multi-class skin lesion detection	DenseNet201, ELM classifier	ISBI2016	93.0	The detection rate is very low in [28], a problem addressed through ICSO-based segmentation.	It lacks the capability to tailor diagnoses to specific patient characteristics.
[29]	Fungal skin disease classification	CNN-MobileNetV2 and ResNet 50	Dr. Gerbi Medium Clinic	93.3	In [29], they do not consider the misclassification rate, which is solved through CD-SNN.	The presence of a relatively higher misclassification rate.

employed for lesion segmentation, resulting in segmented images. Feature extraction involves utilizing both regular pool and fully associated layers, which are combined to generate a feature vector. Goceri [25] introduces a lightweight network architecture made for mobile applications that use color photography to diagnose skin conditions. ShuffleNet, which is known for shuffle channels during convolution to exchange information between classes, does not perform well in classification. Yu and Reiff-Marganiec [26] propose a practical solution for remote skin disease diagnosis applications in the IoT context. The study encompasses two key aspects. The dynamic AI model configuration is presented, which is supported by an IoT-Fog-Cloud distant diagnosis building and exemplified through hardware implementations. An evaluation survey is conducted to assess the performance of machine learning models for skin disease identification. Srinivasu et al. [27] propose a computerized approach for classifying skin diseases using deep learning techniques, specifically MobileNet V2 and LSTM. The MobileNet V2 model is chosen for its efficiency and accuracy, making it suitable for deployment on lightweight computational devices. The model efficiently retains stateful information, enabling precise predictions.

Khan et al. [28] offer a crossover skin condition classification method that blends a 16-layer CNN model with high-layered contrast change-based framework. The multiple images produced by the CNN model are combined with the HDCT technique's sectioned RGB image. The pre-trained DenseNet201 model is fitted to images of fragmented lesions using transfer learning. A stochastic neighbor-nailing approach is used to assess the discarded features of the two entirely associated layers. Nigat et al. [29] present a CNN-based approach for the classification of four common forms of fungal skin diseases. The studies were designed to obtain ideal performance, and it was discovered that an image size of 224 224, ReLU, and RGB color channel may achieve an accuracy of 93.3%. The CNN model is compared to similar structures such as MobileNet V2 and ResNet 50.

III. MATERIALS AND METHODS

Traditional methods of detecting skin problems are fraught with difficulties and limitations, resulting in erroneous and inaccurate diagnoses. Different specialists may decode and analyze a skin issue differently. Dermatologists may have limited knowledge, particularly in remote or underdeveloped areas. This limitation hinders access to specific

disease examinations and treatments. Misdiagnoses and false negatives are also causes for concern, as human error and the intricate nature of individual skin illnesses can lead to misdiagnosis or misinterpretation [38]. By relying on huge datasets, such calculations may overlook critical information for accurate analysis. These models discern specific requirements by learning from particular data sources, enabling them to familiarize themselves with the signs of various skin diseases. Since ML and DL algorithms have access to more detailed skin images, their accuracy will improve over time [39]. Because of their scalability and accessibility, ML and DL models can be used in a variety of healthcare applications, including locations with limited access to dermatologists. They can conduct basic tests, assist general practitioners, and facilitate telemedicine consultations, thereby enhancing access to quick and accurate diagnoses. Challenges in ML/DL techniques for skin disease detection include limited and imbalanced datasets, a lack of interpretability in deep neural networks, sensitivity to variations in image quality, limited generalizability to diverse populations, ethical and privacy concerns, and the need for proper validation and evaluation in clinical practice. To address these issues, the proposed framework is intended to do the following:

- Utilizes data preprocessing to increase the quantity of input data and mitigate the dataset's data imbalance problem;
- Optimizes the segmentation process to accurately capture the target portion, thereby achieving the highest detection rate;
- Introduces the feature optimization technique to select the best features by addressing data dimensionality issues.
- Utilize a deep learning model to classify skin disorders into multiple classes.

A. PROPOSED METHODOLOGY

Figure 1 depicts the conceptual framework of the proposed work, which consists of a series of operations. Patients with skin disorders contribute images to a database depicting various skin conditions relevant to skin disease diagnosis. These images are frequently stored in databases like the ISIC 2017, which serve as useful resources for research and development in this field. Image preprocessing techniques are used to remove undesirable artifacts and improve image quality to ensure accurate analysis. As a result, an improved chameleon swarm optimization (ICSO) algorithm has been designed to accurately recognize and extract the affected area from the images. This facilitates the specific examination and extraction of feature elements from the affected area. Features associated with surface characteristics, variations, and unevenness are isolated from the fragmented region during the mining of the infected section. These features provide critical information about the specific characteristics of the skin condition, aiding in its precise classification and analysis. A multi-strategy seeking optimization (MSSO) algorithm is employed to enhance feature space by eliminating insignificant feature dimensions. Following that, a convolutional deep spiking neural network model makes use of the most significant features. Finally, the test set of images is classified into various categories of skin diseases using the trained CD-SNN model. Through this classification process, common skin conditions such as eczema, psoriasis, vitiligo, melanoma, carcinoma, and blue nevus can be accurately diagnosed, and treatment options can be proposed. This section presents the detailed working process of the proposed method, which includes a series of steps such as data preprocessing and augmentation, target segmentation, feature extraction, feature optimization, detection, and classification.

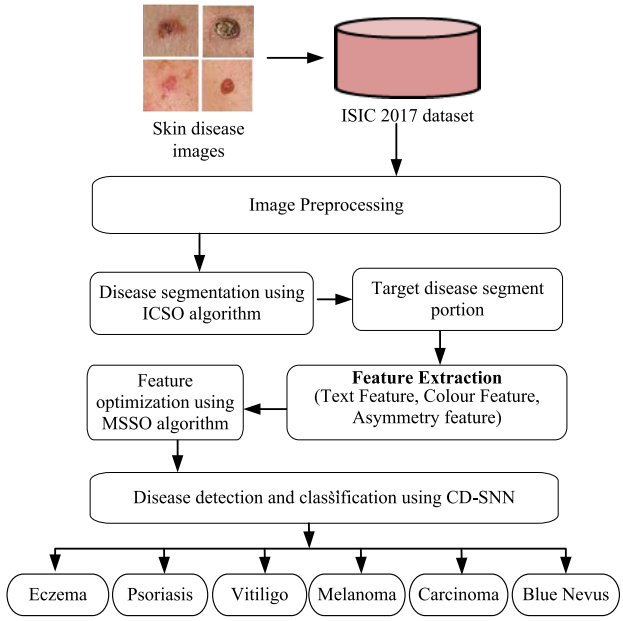

FIGURE 1. Overall conceptual structure of the proposed work.

B. DATA PREPROCESSING AND AUGMENTATION

Data preprocessing plays a crucial role in preparing skin disease images for analysis. It involves several important steps that aim to enhance the quality and suitability of the images for subsequent analysis. The first step in data preprocessing is image cleaning, where techniques such as noise reduction filters or smoothing algorithms are applied to remove unwanted noise and artifacts from the images. This is helpful for reestablishing, by and large, picture quality and lessening the opportunity for a mistaken investigation. Another significant step is picture resizing, which includes changing the size and goal of pictures to a normalized design. This guarantees consistency and lessens computational intricacy during the examination cycle. Resizing procedures, for example, bilinear or bicubic addition, are generally used to resize a picture while saving significant detail. Picture improvement is one more significant part of information preprocessing. Methods such as contrast change,

histogram smoothing, or versatile upgrade strategies are utilized to work on the visual qualities of skin infection pictures. These methods make it all the more likely to imagine significant elements and surfaces, making it simpler to recognize and investigate explicit skin conditions. At long last, district of interest extraction is performed to concentrate and concentrate significant areas of skin infection pictures. This step consists of distinguishing and eliminating areas of skin sores or anomalies of interest. By excluding these areas, further examination can be performed more precisely and productively.

Data augmentation methods are normally utilized in skin disorder image analysis to expand the size and variety of the collection, which can build the vigor and disentanglement of the models. The following information-scaling techniques are frequently used: pivot, scaling, equal flip, and vertical flip. Pivot includes turning the picture through a convincing point, like 90 degrees or 180 degrees. This assists with distinguishing contrasts in the direction of skin sores, which can be helpful for preparing models to be pivot-invariant. Scaling includes increasing or decreasing a picture equally or unevenly. This assists with reenacting various degrees of nearness to a skin sore, which can be helpful for preparing models to perceive and group injuries at various scales. Vertical flip includes reflecting the picture along the upward pivot, while vertical flip includes reflecting the picture along the straight hub. These techniques assist with making variations in the appearance and area of skin sores, permitting models to gain according to alternate points of view and directions. By applying these data augmentation techniques, the informational collection is really extended with new variations of the initial images. This can help overcome the restrictions of the predetermined number of images accessible and reduce the chance of overfitting when the model turns out to be excessively specific for the training data.

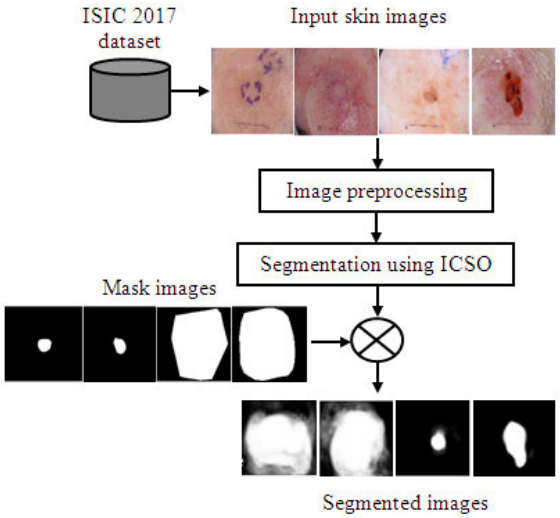

FIGURE 2. Process of skin disease segmentation.

C. TARGET SKIN DISEASE SEGMENTATION

Improved chameleon swarm optimization (ICSO) is a technique used to cluster skin diseases using clinical imaging. Segmentation plays a key role in identifying evidence and the significance of explicit areas of interest in the image, such as skin cancers or affected areas. The ICSO algorithm uses standards of cross-disciplinary expertise to enhance the division cycle and is inspired by how the chameleon species behaves. It will most likely improve the visual impact and accuracy of the segmentation by iteratively adjusting boundaries and guiding to find optimal combinations. It combines the beneficial characteristics of a chameleon's ability to adapt to its present situation with a multitude of insights. The algorithm begins with an underlying populace of potential arrangements (chameleons), which goes through a progression of cycles. Each chameleon evaluates its fitness based on predefined criteria, such as similarity to ground truth or consistency of segmented regions. During the optimization process, chameleons interact with each other, sharing information and updating their positions based on local and global search strategies. As shown in Figure 2, this collaboration allows the algorithm to explore the solution space effectively and converge towards a more accurate segmentation result. In a d-layered searching space, every chameleon addresses the solution for the target segment portion, so we can characterize a two-layered n×d layered y lattice as populace of chameleons.

$$b_t^H = \left[b_{t,1}^H, b_{t,2}^H, \ldots b_{t,d}^H\right] \tag{1}$$

where H equals 1, 2, 3, Iterations with valid positions for the d-th dimension are q and T. The following is a mathematical model that can be used to optimize the behavior and movement of chameleons in search of food.

$$b_{t+1}^{H,G} = \begin{cases} b_t^{H,G} + X_1\left(x_t^{H,G} - j_t^G\right)R_2 + X_2\left(j_t^G - x_t^{H,G}\right) \\ \qquad R_1 R_h \geq x_X \\ b_t^{H,G} + \mu\left(U^G - L^G\right)(R_3 + L_N^G)\mathrm{sgn}\,(Rand - 0.5) \\ \qquad R_H < x_X \end{cases} \tag{2}$$

Here, $b_{t+1}^{H,G}$ is the novel location of the H-th dilettante in the iteration step's G-th dimension. The chameleon's current state at the G-th iteration of iteration T. j_t^G represents the best position any chameleon has ever held in the G-th measurement in the T-th repetition. The R_H, an uniform random number indexed from 0 to 1. For this reason, the length of the tongue can be increased by two times, which should update the position of the chameleon.

$$V_{t+1}^{H,G} = \omega V_t^{H,G} + C_1\left(j_t^G - b_t^{H,G}\right)R_1 + C_2\left(x_t^{H,G} - b_t^{H,G}\right)R_2 \tag{3}$$

where $V_{t+1}^{H,G}$ characterizes the new rapidity of the trimmer in J. In iteration, size T+1 signify the current speed of $V_t^{H,G}$. $\omega V_t^{H,G}$ represents the chameleon's ideal spot in the T-th

dimension. $x_t^{H,G}$ is the current chameleon's most popular area and j_t^G is the most popular circle molded position at any point perceived to chameleons, R_1 and R_2 is the current chameleon's $x_t^{H,G}$ most popular position C_1 and C_2 is the best worldwide position at point perceived to chameleons, and j_t^G are the two positive constants controlling the impact of and falls into the chameleon's tongue and is two erratic measurements dispersed some place in the scope of 0 and 1, $x_t^{H,G}$ and $j_t^G\omega$ is the inertial sub-instance. Assuming we add the past change to this part, the turn frameworks of the comparing tomahawks are communicated in R.

$$V = r\left(\Phi, b_t^{H,G}\right) \tag{4}$$

The rotation matrix V can be described as an accurate perfect as shadows, where 8 is used to represent it.

$$\Phi = R\text{sgn}(rand - 0.5) \times 180 \tag{5}$$

where R is a generated accidental amount between 0 and 1. The measure functions' weight factors (−2) are also added as product to the pairs of objective functions.

$$of_{11} = \sum_{H=1}^{Q}\left(\frac{wC_1}{directivity_H}\right)^2 \tag{6}$$

$$of_{12} = \sum_{H=1}^{Q}\left(\frac{wC_2}{-S11_H}\right)^2 \tag{7}$$

We define the objective function of optimal solution pair, modified from the exponential perfect, is as shadows:

$$of_{21} = \sum_{H=1}^{Q} ZC_1 * E^{-directivity_H} \tag{8}$$

$$of_{22} = \sum_{h=1}^{B} Wd_2 * E^{T11_h} \tag{9}$$

A pair of goal capabilities fitted to a Fourier model is characterized as follows.

$$of_{31} = \sum_{H=1}^{Q} ZC_1 * \cos(directivity_H) \tag{10}$$

$$of_{32} = \sum_{H=1}^{Q} ZC_2 * \cos(S11_H) \tag{11}$$

where H = 1, 2, . . ., 4 each addresses the thunderous recurrence. The first is gotten by social event the sets of not entirely settled in itself and is characterized as follows.

$$\cos t_1 = of_{G1} + of_{G2}G = 1, 2, 3 \tag{12}$$

To provide a general comparison of the objective functions, the following definition of a second cost function is provided.

$$\cos t_2 = \sum_{H=1}^{Q}\frac{ZC_1}{directivity_H} + \frac{ZC_2}{-S11_H}, H = 1, 2, \ldots .4 \tag{13}$$

The working process of optimal segmentation using ICSO is outlined in Algorithm 1.

Algorithm 1 Optimal Segmentation Using ICSO

Input: Number of images, ground truth images, maximum iteration

Output: Target disease portion-segment

1 Initialize the random populace
2 If we describe it as a vector: $b_t^H = \left[b_{t,1}^H, b_{t,2}^H, \ldots b_{t,d}^H\right]$
3 If i=0, j=1
4 While **Do**
5 Define revolution mediums on the pertinent axis are articulated with R.
$V = r\left(\mathbf{\Phi}, b_t^{H,G}\right)$
6 Compute power model using
$of_{11} = \sum_{H=1}^{Q}\left(\frac{wC_1}{directivity_H}\right)^2$
7 If not discard then
8 Compute objective function
$\cos t_2 = \sum_{H=1}^{Q}\frac{ZC_1}{directivity_H} + \frac{ZC_2}{-S11_H}, H = 1, 2, \ldots .4$
9. End if
10 Update the final values
11 End

D. FEATURE EXTRACTION

Feature extraction is critical step, where relevant information is extracted from medical images to characterize different skin conditions. Texture, color, and asymmetry are common features used in this process [30]. Texture refers to the spatial arrangement of pixels in an image and provides information about the surface characteristics of skin lesions. Various texture analysis techniques, such as gray-level co-occurrence matrix (GLCM) [31] and local binary patterns (LBP) [32] are employed to quantify the textural properties of skin lesions. These methods capture patterns, variations, and structures in the image, which can be indicative of specific skin diseases. Color is an essential visual cue in skin disease analysis as different skin conditions often exhibit distinct color variations. The distribution and strength of various features like RGB or HSV in the affected region are included in variation-based feature extraction [33]. Statistical measures, such as the mean, standard deviation, and histograms, are commonly used to summarize data and classify different categories of skin disorders [34]. Nonuniform distribution signifies the variation between the different angles of a lesion or skin region [35]. In the treatment of skin diseases, unevenness can help distinguish between moderate and dangerous lesions. Possible abnormalities can be identified by examining unusual features of skin lesions, such as contrasts in shape, surface, and variance. Shape-based descriptors, such as balancing ratios or shape assessment, can be used to assess skin imbalance. As shown in Figure 3, a full view of skin lesions can be obtained by recognizing surface, diversity, and dispersion features. These features offer a variety of information that can be used in clustering algorithms to distinguish between various types of skin disorders and aid in a precise diagnosis and treatment plan.

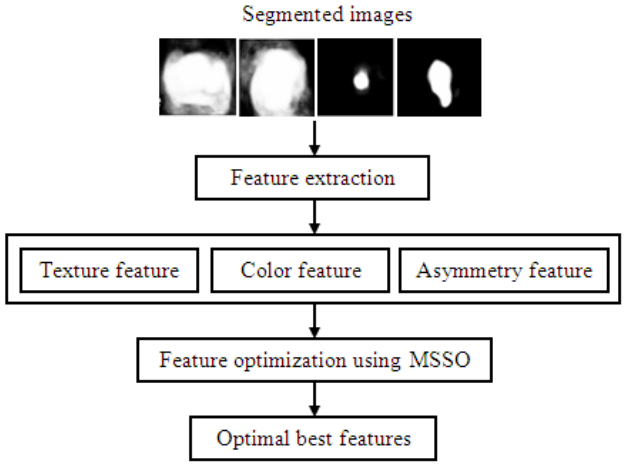

FIGURE 3. Process of feature extraction and optimization.

E. FEATURE OPTIMIZATION

Feature optimization is the process of selecting and preparing features from a given set of data elements to work on the mathematical representation of an AI model. MSSO (multi-strategy seeker optimization) is an algorithm that can be used for optimization. MSSO is a metaheuristic development strategy inspired by the behavior of chameleons in a city which combine various hunting techniques to effectively learn and maximize hunting space.MSSO can be used to find an optimum subset of features that increase the visual appearance of a skin disease location when it comes to incorporating improvement. The algorithm employs multiple techniques, for example, irregularity study, neighborhood search, and universal search, to iteratively assess distinct subsets of elements and modify the arrangement based on the results. MSSO examines the quality of different feature subsets during the optimization process using an objective function that measures the model's classification performance. The algorithm dynamically adjusts its search behavior by adaptively switching between different search strategies based on the exploration-exploitation trade-off. The egotistic measurement can yield the direction, $\overrightarrow{F}_{H,E}(T)$ the altruistic direction, $\overrightarrow{F}_{H,M}(T)$ and the preventative H-separation direction $\overrightarrow{F}_{H,x}(T)$

$$\overrightarrow{F}_{H,E}(T) = \overrightarrow{X}_{H,Best} - \overrightarrow{P}_H(T) \tag{14}$$

$$\overrightarrow{F}_{H,M}(T) = \overrightarrow{J}_{H,Best} - \overrightarrow{P}_H(T) \tag{15}$$

$$\overrightarrow{F}_{H,x}(T) = \overrightarrow{P}_H(T_1) - \overrightarrow{P}_H(T_2) \tag{16}$$

To determine search focusing on, the web index employs an irregular weighted average technique.

$$\overrightarrow{F}_H(T) = sign(\omega \overrightarrow{F}_{H,x}(T) + \psi_1 \overrightarrow{F}_{H,E}(T) + \psi_2 \overrightarrow{F}_{H,M}(T)) \tag{17}$$

here, T, T1, T2, $\overrightarrow{P}_H(T_1)$ and $\overrightarrow{p}_h(s_2)$ are superior to $\overrightarrow{P}_H(T-2)$, $\overrightarrow{P}_H(T-1)$, $\overrightarrow{P}_H(T)\}$ each other; $J_{H,best}$ is the authentic ideal situation in the local where the H-th search component is found; $X_{H,best}$ ideal area from the h-th search component to the ebb and flow area; and [0, 1] are random numbers. ω is the inertial weight. A Gaussian conveyance capability is utilized to depict the size of the hunt step.

$$\mu(\alpha) = E^{-\frac{\alpha^2}{2\delta^2}} \tag{18}$$

where α and δ are the boundaries of the enrollment capability. Be that as it may, this record contains μ_{Max} set to 0.9 to speed up the convergence speed and obtain a suitable individual for the uncertain step size.

$$\mu_H = \mu_{Max} - \frac{S - h_H}{T - h}(\mu_{Max} - \mu_{Min}), \quad H = 1, 2, \ldots S \tag{19}$$

$$\mu_{H,G} = Rand(\mu_H, 1), G = 1, 2, \ldots d \tag{20}$$

Here h_H is the ongoing individual's $P_H(T)$ stream count, requested from most elevated to least movement esteem. In any division, $(\mu_H, 1)$ the scar function is a real number $[\mu_H, 1]$. The size is determined in light of the g-layered search space as follows.

$$\alpha_{\mathrm{HG}} = \delta_{\mathrm{HG}}(\mathrm{T}) - \sqrt{-\ln(\mu_{\mathrm{HG}})} \tag{21}$$

where, δ_{HG} is a structure of the Gaussian distribution, which is calculated as follows.

$$\delta_{HG} = \omega P * ABS(\overrightarrow{P}_{Min} - \overrightarrow{P}_{Max}) \tag{22}$$

Here, ω is the inertial weight. As the evolutionary algebra increases, ω decreases linearly from 0.9 to 0.1. $\overrightarrow{P}_{Min}$ and $\overrightarrow{P}_{Max}$ are the minimum and maximum value variation of the function, respectively. After receiving the person's scout direction and scout step measurements, a location update is indicated.

$$P_{HG}(T+1) = P_{HG}(T) + \alpha_{HG}(T) F_{HG}(T)$$
$$H = 1, 2, \ldots .S; G = 1, 2, \ldots .d \tag{23}$$

where searcher H and G denotes the independent value $F_{HG}(T)$ nd $\alpha_{HG}(T)$ are the searchers direction for the search and the step to the size of the search time T, $P_{HG}(T)$ and $P_{HG}(T+1)$ respectively, and (T + 1), denotes the site and fixed the range X∈ [0, 1] is probability of the probe being fixed by P_H the triple black hole system and the status is calculated as follows.

$$P_{HG}(T+1) = \begin{cases} (Jbest(T) + P_{Min})/2 + RR_3, & L_1 > X_1 \\ Jbest(T) + RR_3 & X_2 \le L_1 X_1 \\ (Jbest(T) + P_{Max})/2 + RR_3, & L_1 < X_2 \end{cases} \tag{24}$$

where: H denotes the H^{th} individual and g denotes the dimension $Jbest(T)$ and the T is the optimal solution to the entire population P_{Max}/P_{Min} is the upper/lower bound of the search region, a fixed range, $X_1, X_2 \in [0, 1]$, and $X_1 < X_2$, R_3 The termination strategy is adopted in the random value

for each dimension K∈ [0, 1]. If k ≤ XX, and the fixed range XX∈ [0, 1].

$$P_{HG}(T+1) = P_{HG}(T) + (1 + \psi R_4) \tag{25}$$

Here: ψ is the measure of interference, R_4 is a random number [−1,1]. Since the position of the searchers is reset, they are randomly distributed around, $Jbest(T)$ the probability of deviating from the local optimum, i.e.

$$|f_J(T+1) - f_J(T)| < 0.01 \cdot |f_J(T+1) \tag{26}$$

$$P_{HG}(T+1) = (Jbest'(T+1) + Jbest(T)) \cdot R_M \tag{27}$$

where: $f_J(T)/f_J(T-1)$ are the upsides of the qualities relating to the worldwide individual optimality of the gathering $T/T-1$, and is an irregular number [−1, 1]. $Jbest'(T+1)$ is the ongoing ideal clarification for the $T+1$ companion. The means associated with upgrading capabilities using the MSSO algorithm is shown Algorithm 2.

Algorithm 2 Feature Optimization Using MSSO

Input: Number of features, maximum iteration and termination condition

Output: Optimal best features

1 Initialize the random population
2 Define the random prejudiced normal to obtain the search alignment.
$\overrightarrow{F}_H(T) = sign(\boldsymbol{\omega}\overrightarrow{F}_{H,x}(T) + \boldsymbol{\psi}_1\overrightarrow{F}_{H,E}(T) + \boldsymbol{\psi}_2\overrightarrow{F}_{H,M}(T))$
3 If i=0, j=1
4 While Do
5 Generate the search direction
6 Addition the triple black hole system
7 If not discard then
8 The Gaussian distribution function is $\boldsymbol{\mu}(\boldsymbol{\alpha}) = E^{-\frac{\alpha^2}{2\delta^2}}$
9 Perform location update
$P_{HG}(T+1) = P_{HG}(T) + \boldsymbol{\alpha}_{HG}(T)[scale = 0.98]F_{HG}(T)H = 1, 2, \ldots .S; G = 1, 2, \ldots .d$
10 Compute possibly jump out of local optimality
$|f_J(T+1) - f_J(T)| < 0.01 \cdot |f_J(T+1)$
11 Find the best output values
12 End if
13 End

F. SKIN DISEASE DETECTION AND CLASSIFICATION

Finally, the Convolutional Deep Spiking Neural Network (CD-SNN) model is employed to classify test images into specific categories of skin diseases. This classification process plays a crucial role in accurately identifying common skin diseases such as Eczema, Psoriasis, Vitiligo, Melanoma, Carcinoma, and Blue Nevus. By applying the CD-SNN model to the testing images, we can obtain reliable predictions and assist in making informed decisions regarding diagnosis and treatment. The CD-SNN model leverages its learned knowledge and understanding of skin disease patterns and features to classify the testing images. Each image is analyzed and compared to the patterns and characteristics learned during the training phase. Based on these comparisons, the CD-SNN model assigns the testing images to specific skin disease categories with a high degree of accuracy. As shown in Figure 4, by automating the classification process through the trained CD-SNN model, the diagnosis of skin diseases becomes more efficient and reliable, leading to improved patient care and outcomes. The proposed CD-SNN algorithm's basic algebraic equations for the scaling function and activation function are derived as follows:

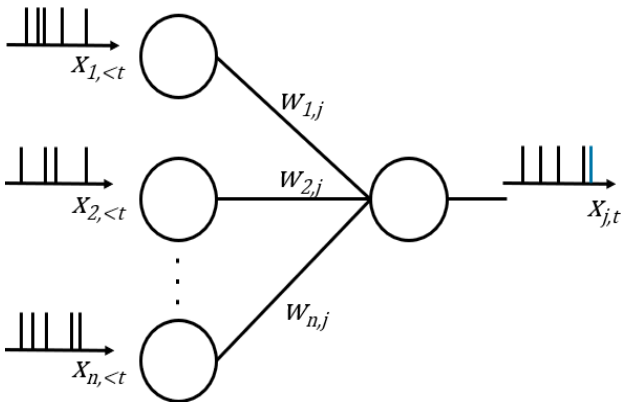

FIGURE 4. Process of SNN model.

Let f denote the wavelet frequency over which the empirical wavelet transforms (EWT) should be decomposed. Its Fourier transform is denoted as $\hat{f}$, and its inverse Fourier transform is denoted as $\hat{f}$. In signal space $l^2(r)$, the empirical frequency spectrum $\hat{\psi}_q(\delta)$ and the empirical scaling function spectrum $\hat{\psi}_b(\delta)$ can be expressed mathematically as:

$$\hat{\psi}_q(\delta) = \begin{cases} 1 & if (1-\eta)\delta_q \le (1-\eta)\delta_{q+1} \\ \cos\left[\frac{\pi}{2}\beta\left(\frac{2}{2\eta\delta_{q+1}}(|\delta_q| - (1-\eta)\delta_{q+1}\right)\right] & \\ \quad if (1-\eta)\delta_{q+1} \le |\delta_q| \le (1+\eta)\delta_{q+1} & \\ \sin\left[\frac{\pi}{2}\beta\left(\frac{2}{2\eta\delta_q}(|\delta_q| - (1-\eta)\delta_q\right)\right] & \\ \quad if (1-\eta)\delta_q \le |\delta_q| \le (1+\eta)\delta_q & \\ 0 \quad otherwise & \end{cases} \tag{28}$$

$$\hat{\varphi}_q(\delta) = \begin{cases} 1 & if\ |\delta| \le (1-\eta)\delta_q \\ \cos\left[\frac{\pi}{2}\beta\left(\frac{2}{2\eta\delta_q}(|\delta_q| - (1-\eta)\delta_q\right)\right] & \\ \quad if\ (1-\eta)\delta_q \le |\delta| \le (1+\eta)\delta_q & \\ 0 \quad otherwise & \end{cases} \tag{29}$$

In the above, is the q-th most noteworthy of the Fourier range, $\boldsymbol{\eta} \in [\mathbf{0}, \mathbf{1}]$. The reason (P) ∈ $\boldsymbol{Ck}$ ([**0**, **1**]) is usually used as follows:

$$\beta(P) = \begin{cases} 0 & if\ P < 0 \\ P^4(35 - 84P + 70P^2 - 20P^3) & \\ \quad if\ P \in [0, 1] & \\ 1 & if\ P > 1 \end{cases} \tag{30}$$

The inner product is used to calculate the specific coefficients between empirical wavelets and signals, which is similar to how the traditional wavelet transform is built.

$$W_f^{\varepsilon}(q,\ T)=\langle f,\ \psi_q\rangle=\int f(\tau)\overline{\psi_q(\tau-T)D\tau}\ \ \left(\hat{f}\ (\delta)\ \overline{\hat{\psi}_q(\delta)}\right)^V \tag{31}$$

where $\tau \mathrm{N} = \eta{\cdot}\delta\mathrm{N}$ is the half length of the progress stage. Besides, the assessed coefficients between the observational motions and the not entirely set in stone by the internal item scale capability as follows:

$$W_f^{\varepsilon}(0,\ T)=\langle f,\ \varphi_1\rangle=\int f(\tau)\overline{\varphi_1\ (\tau-T)D\tau}\ \ \left(\hat{f}\ (\delta)\ \overline{\hat{\varphi}_1(\delta)}\right)^V \tag{32}$$

We define the decomposed signal and final experiential mode, is uttered as follows:

$$F_K=\begin{cases} Z_f^{\varepsilon}(0,T)\otimes\varphi_1\ (T) & if\ K=0 \\ Z_f^{\varepsilon}(q,T)\otimes\psi_q\ (T) & if\ K>0 \end{cases} \tag{33}$$

Let p^T be the K^{th} subseries-generated input trajectory at time S. The inform gate at time S is determined by the contribution and activation at time *T-1*.

$$Z_{Gate}^T=\sigma(W_z\cdot p^T+u_z\cdot i_{State}^{T-1}) \tag{34}$$

where W_z and u_z the weight matrices Z_{Gate}^T and i_{State}^{T-1}, respectively. An update gate Z_{Gate}^T determines how much a GRU unit refreshes its substance or execution, and is like a LSTM unit entryway that takes a straight total between the new information and the present status. The reset gate, just like the update gate, is calculated as follows:

$$r^T=\sigma(W_z\cdot p^T+u_z\cdot i_{State}^{T-1}) \tag{35}$$

Through reset entrance as r^T, the applicant activation $\tilde{i}^T$ is calculated as follows:

$$\tilde{i}^T=\tan i(W\cdot p^T+u(r^T\Theta i_{State}^{T-1})) \tag{36}$$

In the abovementioned, W and U are the comparing weight frameworks, and $\odot$ is the basic abundance. Also, r^T it indicates whether the update $\tilde{i}^T$ is considered the last one implemented i_{State}^{T-1}. Here $r^T \rightarrow \mathbf{0}$, the remaining gate GRU units are constructed without experience and experience $r^T = \mathbf{1}$, the up-and-comer enactment definition deteriorates to the essential RNN competitor actuation detailing. At long last, the transient enactment of the GRU unit is register by direct addition between the applicant initiation and the past actuation as follows.

$$i^T=(1-Z_{Gate}^T)\cdot i_{Gate}^{T-1}+Z_{Gate}^T\cdot\tilde{i}^T \tag{37}$$

The error series represents $Error_k(T) = i_k(T) = F_k(T)$ the actual $f_K(T)$ observation at time S and $i_k(S)$ the anticipated result at time S acquired by the GRU model. Allow the information be a spiking to prepare. In this paper, the Maximum Pooling strategy is embraced, for this situation, hands down the biggest elements of recently executed secret impacts are held. The maximum pool can be modeled as follows with depth c in the previous feature graph:

$$b_{A'',q''}^D=Max(P_H),\ P_H\in hfmhfm_{A',q'}^D \tag{38}$$

where A' and q' are the extents of the info ear map for the HFM, and A'' and q'' are the extents of the creation of the maximum combining process. The steps associated with the course of skin disease discovery and arrangement utilizing CD-SNN is summed up in Algorithm 3.

Algorithm 3 Skin Disease Detection and Classification Using CD-SNN

Input: Optimal best features, ground truth images, training and testing set

Output: Classes-Eczema, Psoriasis, Vitiligo, Melanoma, Carcinoma, and Blue Nevus

1 Initialize the random population
2 Define inner product with a scaling function
$W_f^{\boldsymbol{\varepsilon}}(0,T)=\langle f,\boldsymbol{\varphi}_1\rangle=\int f(\boldsymbol{\tau})\overline{\boldsymbol{\varphi}_1(\boldsymbol{\tau}-T)D\tau}$
$\left(\hat{f}\ (\boldsymbol{\delta})\ \overline{\hat{\varphi}_1(\boldsymbol{\delta})}\right)^V$
3 If I =0, j=1
4 While **Do**
5 Compute candidate activation
$\tilde{i}^T=\tan i(W\cdot p^T+u(r^T\Theta i_{State}^{T-1}))$
6 Perform energy updates
$Dv_M(T)=DT\tau_{mem}((V_{Leak}-V_M(T))+h_{syn}^M(T))$
7 If not discard **then**
8 Define convolutional layer
$hfm^{(1)}=F(W^{(1)}*a_{A,q}+bias^{(1)})$
9 Find the best output value
10 End if
11 End

IV. RESULTS AND DISCUSSIONS

This section focuses on reporting the findings and comparing the proposed CD-SNN technique to existing skin disease detection techniques. The performance of the CD-SNN technique is validated using the benchmark ISIC 2017 dataset, which is widely used in the field of dermatology. The implementation of the proposed technique is carried out in the Google Colab simulation environment, utilizing the Python programming language. The CD-SNN implementation results are compared to various cutting-edge algorithms, for example, the basic ABCDE rule(asymmetry, border, color, diameter and evolving), the support vector machine (SVM), and data gravitation-based classification with naive Bayes (DGC-NB). The findings of this study provide crucial information on the strengths and weaknesses of the proposed method in comparison to existing methods. This correlation enables the detection of the potential benefits and advancements given by the CD-SNN technique for identifying skin diseases. In general, the results and benchmarking shown in this section demonstrate the significance and adequacy of the CD-SNN approach. By establishing its superiority over

existing methodologies, this study makes a contribution to the field of dermatology and allows for future improvements in the detection and treatment of skin disorders.

A. DATASET DESCRIPTION

The ISIC 2017 dataset, officially known as the International Skin Imaging Collaboration Challenge 2017 dataset, serves as a valuable resource for the evaluation and classification of skin disorders. Specifically designed to advance computer-assisted skin disease research, this publicly available repository features a wealth of dermoscopy images—high-resolution captures of skin lesions obtained through the specialized imaging technique known as dermoscopy. Dermoscopy enables an in-depth examination of the skin, unveiling subsurface and color patterns not visible to the naked eye. The dataset is instrumental in fostering original research, providing detailed descriptions of image properties for various skin diseases. These descriptions play a pivotal role in the construction and evaluation of data models for disease diagnosis. The dataset is characterized by skin disease classes, and its training and test sample sizes are outlined in Table 2 . To ensure standardized inputs for model training and evaluation, the dataset undergoes meticulous preprocessing, encompassing normalization, resizing, label encoding, and data splitting. Additionally, data augmentation techniques such as rotation, flipping, zooming, brightness and contrast adjustments, and shearing are employed to diversify the training set, enhancing the model's robustness and performance. Together, these steps contribute to the effectiveness and reliability of the proposed DermCDSM in the context of skin disease detection and classification. Figure 5 shows test images from each skin disease class in the ISIC 2017 dataset. The segmentation results of our suggested ICSO technique are shown in Figure 6.

TABLE 2. Dataset description.

Skin disease class	Original data		Data after augmentation	
	Training	Testing	Training	Testing
Eczema	315	110	12500	7564
Psoriasis	96	55	13659	6895
Vitiligo	214	100	12478	7500
Melanoma	206	105	11235	6500
Carcinoma	110	60	13698	8100
Blue Nevus	185	90	13568	7500
Total samples	1126	520	77138	44059

B. RESULT ANALYSIS OF PROPOSED CD-SNN TECHNIQUE

The results for eczema disease detection in the training case are presented in Figure 7. The training process was conducted over multiple epochs, with each epoch representing a complete pass through the training dataset. In the initial epoch, the accuracy of eczema disease detection is 95.236%, with precision, recall, specificity, and F-measure values of

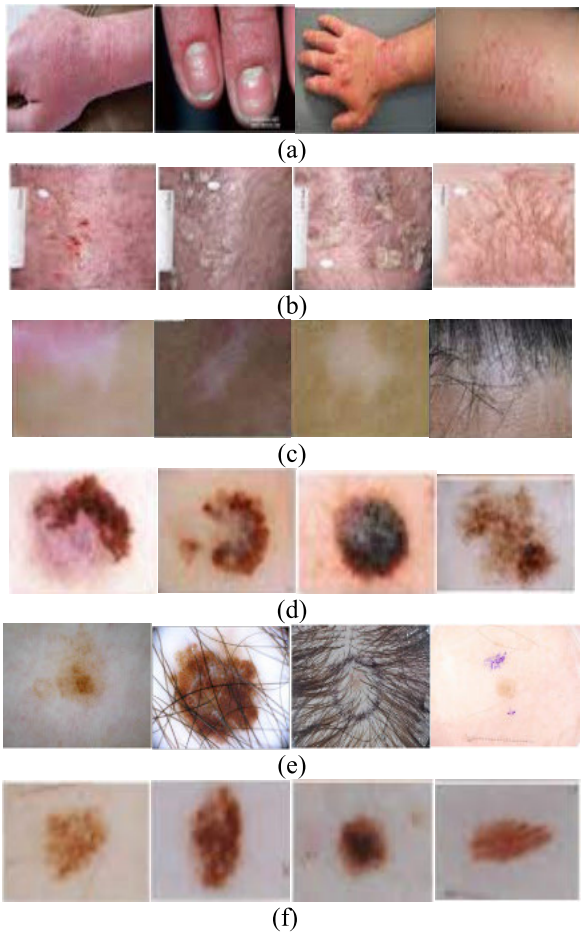

FIGURE 5. Test samples from ISIC 2017 dataset (a) Eczema (b) Psoriasis (c) Vitiligo (d) Melanoma (e) Carcinoma (f) Blue Nevus.

94.896%, 94.875%, 95.031%, and 94.885%, respectively. For the 100th epoch, we observe a performance increase with a precision of 96.348%. Similarly, testing was performed over different epochs, with each stage increasing the total number of test data. In the 100th epoch, we observe a noticeable increase in performance, with a precision of 96.568%. Additionally, accuracy, recall, specificity, and F-measure values improved to 96.124%, 96.090%, 95.744%, and 96.106%, respectively.

When the results of psoriasis detection are studied, it is discovered that there is a steady rise in performance as the number of epochs increases during training. The test phase, like the training phase, was divided into stages, with each stage using a different sample of the test data. Upon analyzing the results, it is observed that there is consistent improvement in performance as the number of epochs increases during the testing phase, as shown in Figure 8.

The learning curve of vitiligo disease is given in Figure 9(a). The accuracy of Vitiligo diagnosis is 95.398% in the initial stage, with precision, recall, specificity, and F-measure values of 95.148%, 95.680%, 94.895%, and 95.413%, respectively. However, this information fluctuates during training. The testing setup, like training, includes

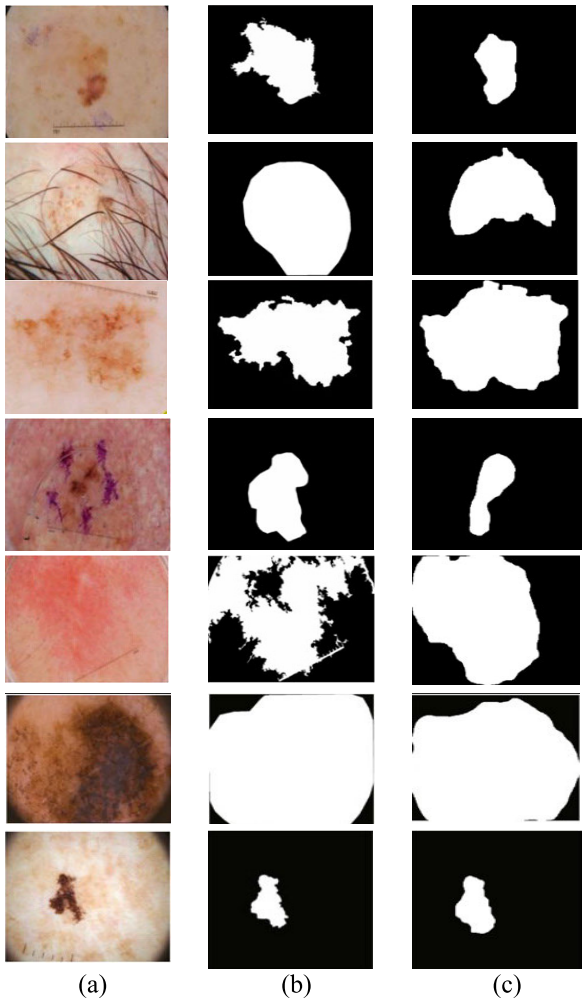

FIGURE 6. Segmentation results (a) test input (original) (b) After transformation (c) segmented output from ICSO algorithm.

various stages and performance indicators. The accuracy of vitiligo detection is 94.978% at the standard, and the scores for precision, recall, specificity, and F-measure are 95.345%, 95.678%, 94.963%, and 95.511%, respectively. By the 100th epoch, the accuracy of vitiligo detection declines to 92.686%. Figure 10 depicts the outcomes of the training and test phases of melanoma disease detection. In the initial stage, melanoma diagnosis detection showcases an accuracy of 96.235%, with precision, recall, specificity, and F-measure values of 96.147%, 95.897%, and 95.978%, respectively. The accuracy of melanoma disease detection improves to 97.182% in the final stage. Upon examining the results, it is observed that the performance metrics continue to improve as the number of epochs increases during the testing phase.

Figure 11 depicts the learning curve for detecting carcinoma. We observe a gradual decline in performance metrics as the number of epochs increases during the testing phase. At the 100th epoch, the accuracy of identifying carcinoma disease has dropped to 92.692%. Similarly, Figure 12 depicts the training and test results for detecting blue nevus disease.

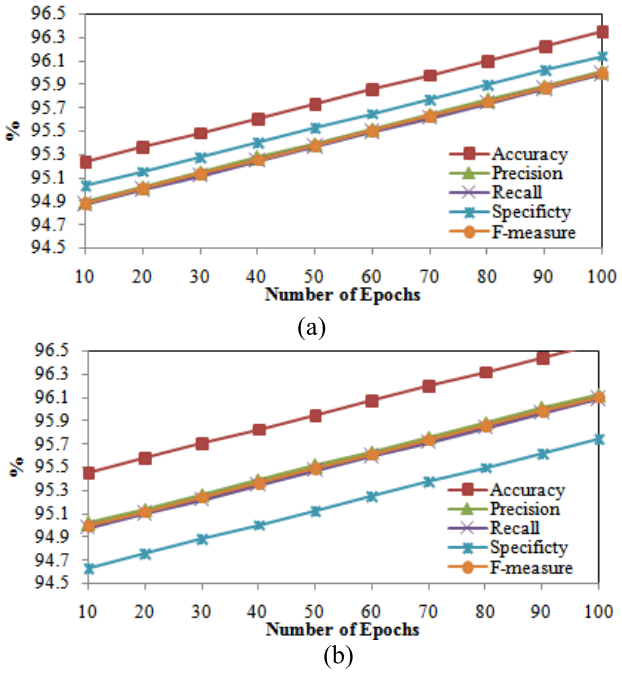

FIGURE 7. Result of Eczema disease detection (a) training case (b) testing case.

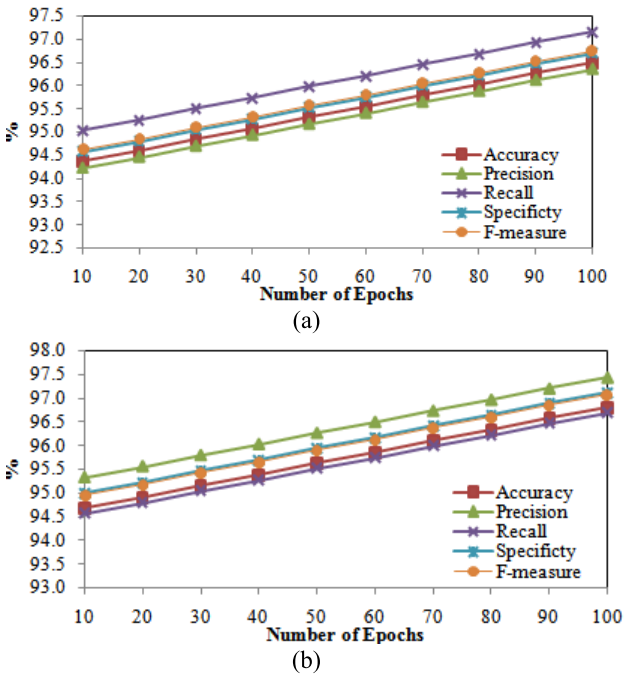

FIGURE 8. Result of Psoriasis disease detection (a) training case (b) testing case.

A small decline is noticed while training. The same trend is also observed during testing.

C. COMPARATIVE ANALYSIS OF PROPOSED AND EXISTING SKIN DISEASE DETECTION TECHNIQUES

Table 3 presents the results of the comparison of different skin disease detection techniques for the ISIC 2017 original dataset. Table 4 presents the results of the comparison of

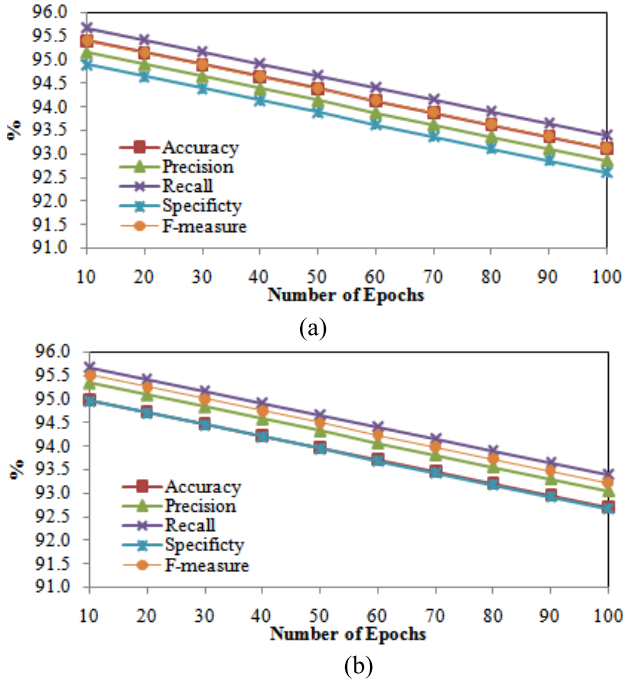

FIGURE 9. Result of Vitiligo disease detection (a) training case (b) testing case.

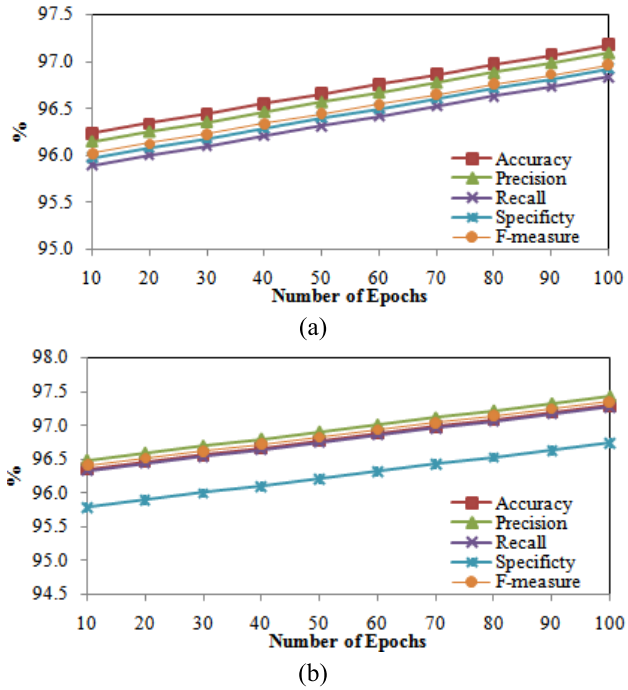

FIGURE 10. Result of Melanoma disease detection (a) training case (b) testing case.

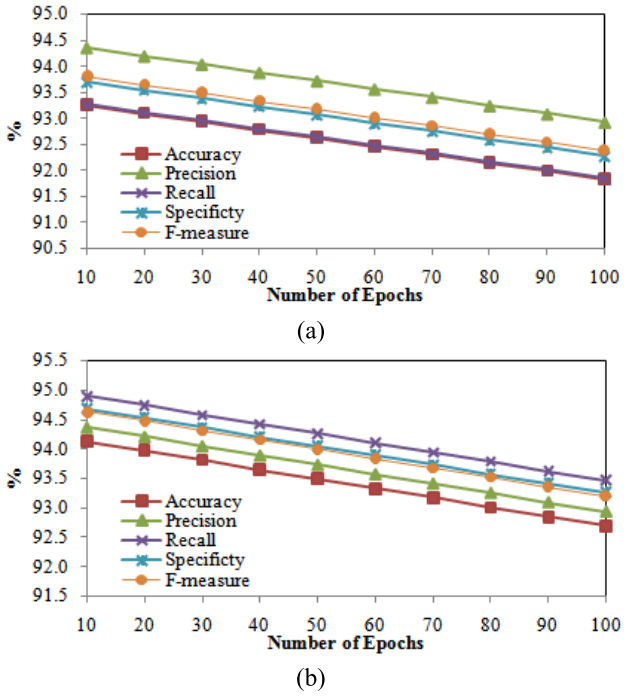

FIGURE 11. Result of Carcinoma disease detection (a) training case (b) testing case.

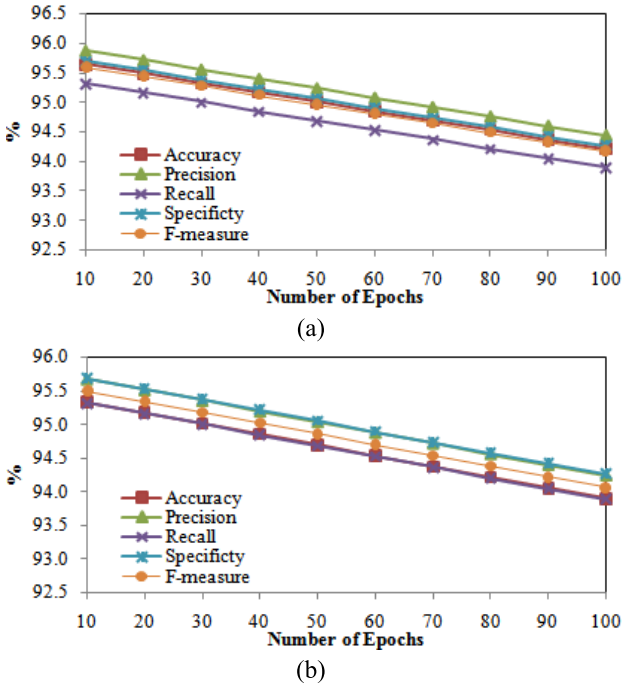

FIGURE 12. Result of Blue Nevus disease detection (a) training case (b) testing case.

different skin disease detection techniques for the ISIC 2017 augmented dataset. Figure 10 shows the comparative analysis of the proposed CD-SNN with existing detection techniques for eczema disease, revealing interesting findings. In terms of accuracy, the CD-SNN technique demonstrates a significant improvement, achieving an increase of 15.955% and 14.955% in the training and testing cases, respectively, compared to the ABCD rule. The accuracy of the CD-SNN approach is improved by 10.970% and 5.985% in the training case and 9.950% and 5.965% in testing, respectively, compared to SVM and DGT-NB. Likewise, the CD-SNN approach significantly improves the estimation of F-measure. It attains an increase of 14.955% and 14.955% in training and testing, respectively, compared to the ABCD rule.

In comparison to SVM and DGT-NB, CD-SNN improves F-measure by 10.970% and 4.985% for training and 9.950% and 5.965% for testing, respectively.

Figure 13 presents a comparative analysis of CD-SNN and existing techniques for psoriasis detection. In terms of accuracy, the CD-SNN method has shown significant improvement, with a respective increase of 19.617% and 18.617% in the quantity of training and experiments when compared to the ABCD rule. Notably, the CD-SNN approach outperforms SVM and DGT-NB in precision, exhibiting improvements of 13.078% and 6.539% in training, and 13.078% and 6.539% in testing, respectively. The CD-SNN technique demonstrates substantial enhancements over current methods, surpassing SVM and DGT-NB with precision improvements of 13.078% and 6.539% in training, and 13.078% and 6.539% in testing, respectively.

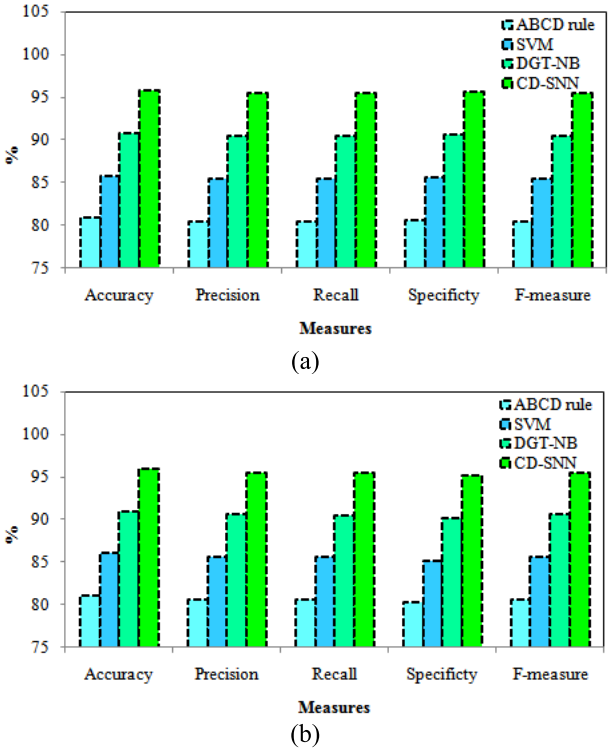

FIGURE 13. Results comparison of Eczema skin disease detection techniques for ISIC 2017 augmented dataset with (a) training case (b) testing case.

Figure 14 shows a performance analysis of CD-SNN in comparison with existing psoriasis detection algorithms. In terms of accuracy, the CD-SNN approach has made significant improvements, with an increase of 19.617% and 18.617% in training and tests, respectively, when compared to the ABCD rule. Also, the CD-SNN technique outperforms SVM and DGT-NB in accuracy by 13.078% and 6.539%, respectively, for training and testing. In the training and testing cases, the CD-SNN outperforms ABCD Rule, SVM, and DGT-NB in terms of precision, recall, and specificity. Furthermore, the CD-SNN approach shows significant gains in F-measure. When compared to the ABCD rule, it achieves

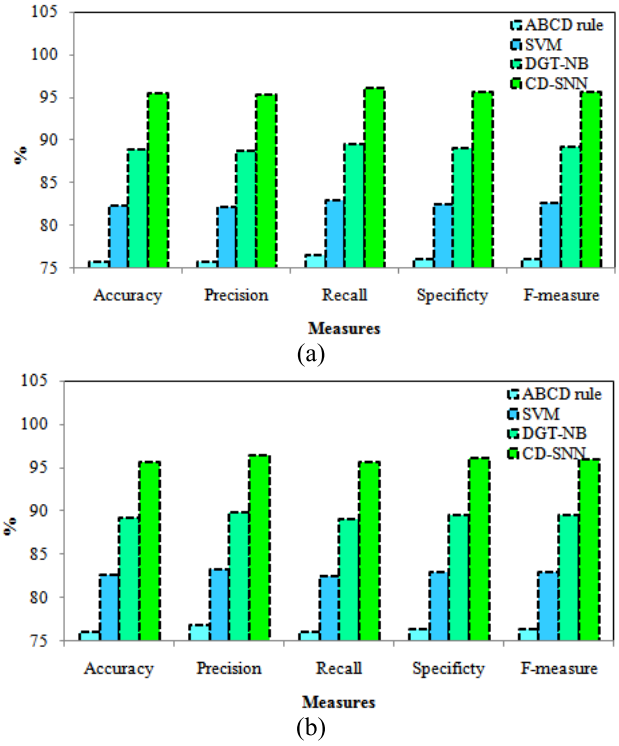

FIGURE 14. Results comparison of Psoriasis skin disease detection techniques for ISIC 2017 augmented dataset with (a) training case (b) testing case.

increases of 19.617% and 18.617% in the training and testing scenarios, respectively. The CD-SNN method excels over SVM and DGT-NB in terms of F-measure increases of 13.078% and 6.539% in the training case and 13.078% and 6.539% in the testing case, respectively.

Figure 15 presents a comparative analysis of proposed and existing detection techniques for Vitiligo disease. The CD-SNN technique demonstrates the highest values for accuracy, precision, recall, specificity, and F-measure among all the techniques, both in the training and testing phases. It outperforms the ABCD rule, SVM, and DGT-NB techniques. While the SVM and DGT-NB techniques show improvements in accuracy, precision, recall, specificity, and F-measure compared to the ABCD rule, the CD-SNN technique exhibits the highest performance across all metrics.

The comparative analysis of proposed and existing detection techniques for Melanoma disease is presented in Figure 16. The CD-SNN technique exhibits the highest values for accuracy, precision, recall, specificity, and F-measure among all the techniques, both in the training and testing phases. It outperforms the ABCD rule, SVM, and DGT-NB techniques. While the SVM and DGT-NB techniques demonstrate improvements in accuracy, precision, recall, specificity, and F-measure compared to the ABCD rule, the CD-SNN technique consistently achieves the highest performance across all metrics.

The comparative analysis of proposed and existing detection techniques for Carcinoma disease is presented

TABLE 3. Comparative analysis of proposed and existing skin disease detection techniques for ISIC 2017 original dataset.

Class	Technique	Training					Testing				
		Accuracy	Precision	Recall	Specificity	F-score	Accuracy	Precision	Recall	Specificity	F-score
Eczema	ABCD rule	86.053	82.295	81.456	79.493	81.873	85.717	84.257	82.929	70.324	83.588
	SVM	87.077	83.318	82.479	80.516	82.896	86.741	85.280	83.952	71.347	84.611
	DGT-NB	88.100	84.342	83.503	81.540	83.920	87.764	86.304	84.976	72.371	85.635
	CD-SNN	89.124	85.365	84.526	82.563	84.943	88.788	87.327	85.999	73.394	86.658
Psoriasis	ABCD rule	86.493	82.166	81.165	79.290	81.662	87.953	86.493	85.165	72.560	85.824
	SVM	87.516	83.189	82.188	80.313	82.685	88.977	87.516	86.188	73.583	86.847
	DGT-NB	88.540	84.213	83.212	81.337	83.709	90.000	88.540	87.212	74.607	87.871
	CD-SNN	89.563	85.236	84.235	82.360	84.733	91.024	89.563	88.235	75.630	88.894
Vitiligo	ABCD rule	86.053	82.295	81.456	79.493	81.873	85.717	84.257	82.929	70.324	83.588
	SVM	87.077	83.318	82.479	80.516	82.896	86.741	85.280	83.952	71.347	84.611
	DGT-NB	88.100	84.342	83.503	81.540	83.920	87.764	86.304	84.976	72.371	85.635
	CD-SNN	89.124	85.365	84.526	82.563	84.943	88.788	87.327	85.999	73.394	86.658
Melanoma	ABCD rule	86.493	82.166	81.165	79.290	81.662	87.953	86.493	85.165	72.560	85.824
	SVM	87.516	83.189	82.188	80.313	82.685	88.977	87.516	86.188	73.583	86.847
	DGT-NB	88.540	84.213	83.212	81.337	83.709	90.000	88.540	87.212	74.607	87.871
	CD-SNN	89.563	85.236	84.235	82.360	84.733	91.024	89.563	88.235	75.630	88.894
Carcinoma	ABCD rule	86.053	82.295	81.456	79.493	81.873	85.717	84.257	82.929	70.324	83.588
	SVM	87.077	83.318	82.479	80.516	82.896	86.741	85.280	83.952	71.347	84.611
	DGT-NB	88.100	84.342	83.503	81.540	83.920	87.764	86.304	84.976	72.371	85.635
	CD-SNN	89.124	85.365	84.526	82.563	84.943	88.788	87.327	85.999	73.394	86.658
Blue Nevus	ABCD rule	86.493	82.166	81.165	79.290	81.662	87.953	86.493	85.165	72.560	85.824
	SVM	87.516	83.189	82.188	80.313	82.685	88.977	87.516	86.188	73.583	86.847
	DGT-NB	88.540	84.213	83.212	81.337	83.709	90.000	88.540	87.212	74.607	87.871
	CD-SNN	89.563	85.236	84.235	82.360	84.733	91.024	89.563	88.235	75.630	88.894

in Figure 17. The CD-SNN technique demonstrates the highest values for accuracy, precision, recall, specificity, and F-measure among all the techniques, both in the training and testing phases. It outperforms the ABCD rule, SVM, and DGT-NB techniques. While the SVM and DGT-NB techniques show improvements in accuracy, precision, recall, specificity, and F-measure compared to the ABCD rule, the CD-SNN technique consistently achieves the highest performance across all metrics.

The comparative analysis of proposed and existing detection techniques for Blue Nevus disease is presented in Figure 18. The CD-SNN technique demonstrates the highest values for accuracy, precision, recall, specificity, and F-measure among all the techniques, both in the training and testing phases. It outperforms the ABCD rule, SVM, and DGT-NB techniques. While the SVM and DGT-NB techniques demonstrate improvements in accuracy, precision, recall, specificity, and F-measure compared to the ABCD rule, the CD-SNN technique consistently achieves the highest performance across all metrics.

D. INTERPRETABILITY OF PROPOSED CD-SNN MODEL

In this study, we employ an innovative approach to enhance the interpretability of the Convolutional Deep Spiking Neural Network (CD-SNN) model in skin disease detection. Utilizing the ISIC 2017 dataset, our proposed methodology incorporates key components aimed at improving both prediction accuracy and the transparency of the decision-making process. The segmentation phase is optimized using the Improved Chameleon Swarm Optimization (ICSO) algorithm, refining the identification of crucial regions associated with skin diseases. Additionally, we address challenges related to data dimensionality through the application of the Multi-Strategy Seeking Optimization (MSSO) algorithm, optimizing feature selection to enhance the relevance of input features for disease detection. The CD-SNN model, known for its proficiency in skin cancer diagnosis and multi-class classification, is employed to further enhance the precision of disease detection. To enhance interpretability, we introduce a dedicated eXplainable Artificial Intelligence (XAI) module into our framework. This module is designed to provide explanations for the predictions made by the CD-SNN model, ensuring transparency in the decision-making process. The integration of XAI techniques facilitates the creation of a comprehensive user interface that presents both the predicted outcomes and corresponding explanations. This user interface serves as a valuable tool for healthcare professionals and users, offering insights into the model's predictions and aiding in the decision-making process. In Figure 19, we showcase the interpretability achieved through the XAI module.

TABLE 4. Comparative analysis of proposed and existing skin disease detection techniques for ISIC 2017 augmented dataset.

Class	Technique	Training					Testing				
		Accuracy	Precision	Recall	Specificity	F-score	Accuracy	Precision	Recall	Specificity	F-score
Eczema	ABCD rule	80.837	80.497	80.476	80.632	80.486	81.057	80.613	80.579	80.233	80.596
	SVM	85.822	85.482	85.461	85.617	85.471	86.042	85.598	85.564	85.218	85.581
	DGT-NB	90.807	90.467	90.446	90.602	90.456	91.027	90.583	90.549	90.203	90.566
	CD-SNN	96.792	95.452	95.431	95.587	95.441	96.012	95.568	95.534	95.188	95.551
Psoriasis	ABCD rule	75.812	75.678	76.475	76.021	76.075	76.121	76.767	76.021	76.441	76.392
	SVM	82.351	82.217	83.014	82.560	82.614	82.660	83.306	82.560	82.980	82.932
	DGT-NB	88.890	88.756	89.553	89.099	89.153	89.199	89.845	89.099	89.519	89.471
	CD-SNN	95.429	95.295	96.092	95.638	95.692	95.738	96.384	95.638	96.058	96.010
Vitiligo	ABCD rule	83.275	83.025	83.557	82.772	83.290	82.855	83.222	83.555	82.840	83.388
	SVM	86.934	86.684	87.216	86.431	86.949	86.514	86.881	87.214	86.499	87.047
	DGT-NB	90.593	90.343	90.875	90.090	90.608	90.173	90.540	90.873	90.158	90.706
	CD-SNN	94.252	94.002	94.534	93.749	94.267	93.832	94.199	94.532	93.817	94.365
Melanoma	ABCD rule	85.761	85.673	85.423	85.504	85.548	85.872	86.004	85.850	85.315	85.927
	SVM	89.410	89.322	89.072	89.153	89.197	89.521	89.653	89.499	88.964	89.576
	DGT-NB	93.059	92.971	92.721	92.802	92.846	93.170	93.302	93.148	92.613	93.225
	CD-SNN	96.708	96.620	96.370	96.451	96.495	96.819	96.951	96.797	96.262	96.874
Carcinoma	ABCD rule	78.839	79.939	78.849	79.278	79.390	79.704	79.946	80.478	80.268	80.211
	SVM	83.407	84.507	83.417	83.846	83.958	84.272	84.514	85.046	84.836	84.779
	DGT-NB	87.975	89.075	87.985	88.414	88.527	88.840	89.082	89.614	89.404	89.347
	CD-SNN	92.543	93.643	92.553	92.982	93.095	93.408	93.650	94.182	93.972	93.915
Blue Nevus	ABCD rule	82.987	83.222	82.673	83.047	82.947	82.675	83.026	82.662	83.035	82.844
	SVM	86.966	87.201	86.652	87.026	86.926	86.654	87.005	86.641	87.014	86.823
	DGT-NB	90.945	91.180	90.631	91.005	90.905	90.633	90.984	90.620	90.993	90.802
	CD-SNN	94.924	95.159	94.610	94.984	94.883	94.612	94.963	94.599	94.972	94.781

TABLE 5. Accuracy comparison of proposed and state-of-art skin disease detection techniques.

Ref.	Classifier	Dataset	Accuracy (%)
[20]	ACNN	ISIC 2017	91.000
[21]	AlexNetandVGG16	Wuhan Union Hospital	89.560
[22]	DRL	Atlas, Dermatoweb	91.730
[23]	ConvNet-Inception-V3	ISIC 2019 and ISIC 2020	86.900
[24]	MASK-RCNN	ISBI2016, ISBI2017	93.600
[25]	Modified-MobileNet	DermWeb	94.760
[26]	TEMCM- MobileNet	HAM10000	94.253
[27]	MobileNet V2 and LSTM	HAM10000	85.000
[28]	DenseNet201-ELM	ISBI2016	92.860
[29]	CNN-MobileNetV2	Dr. Gerbi Medium Clinic	93.300
[30]	DGT-NB	ISIC 2017 Original	72.700
This work	**CD-SNN**	**ISIC 2017 Original**	**89.906**
		ISIC 2017 Augmented	**95.070**

The visualization demonstrates the synergy between our proposed model, incorporating ICSO, MSSO, and CD-SNN, and the XAI module, providing an intuitive representation of the model's decision rationale. The collected data,

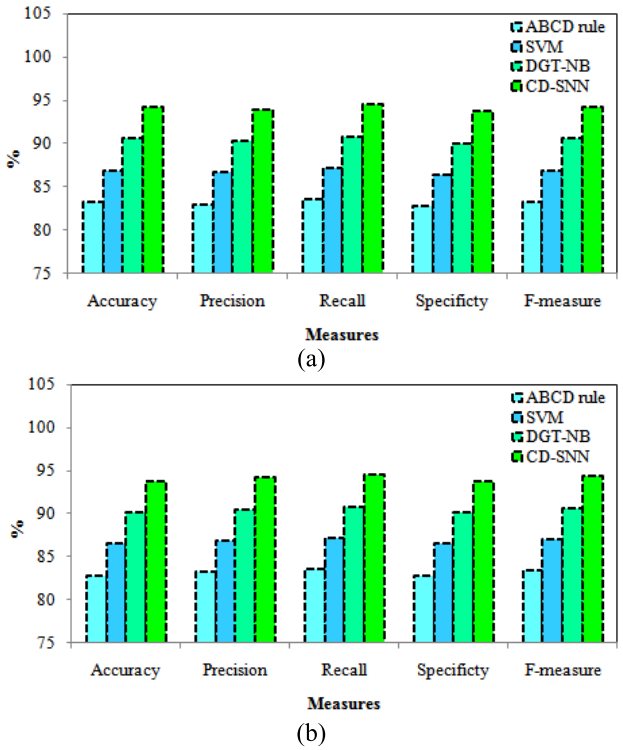

FIGURE 15. Results comparison of Vitiligo skin disease detection techniques for ISIC 2017 augmented dataset with (a) training case (b) testing case.

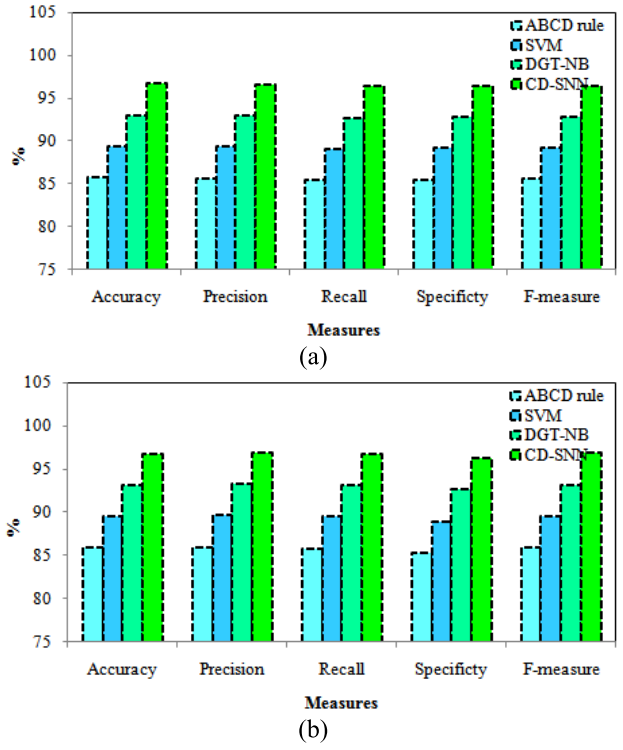

FIGURE 16. Results comparison of Melanoma skin disease detection techniques for ISIC 2017 augmented dataset with (a) training case (b) testing case.

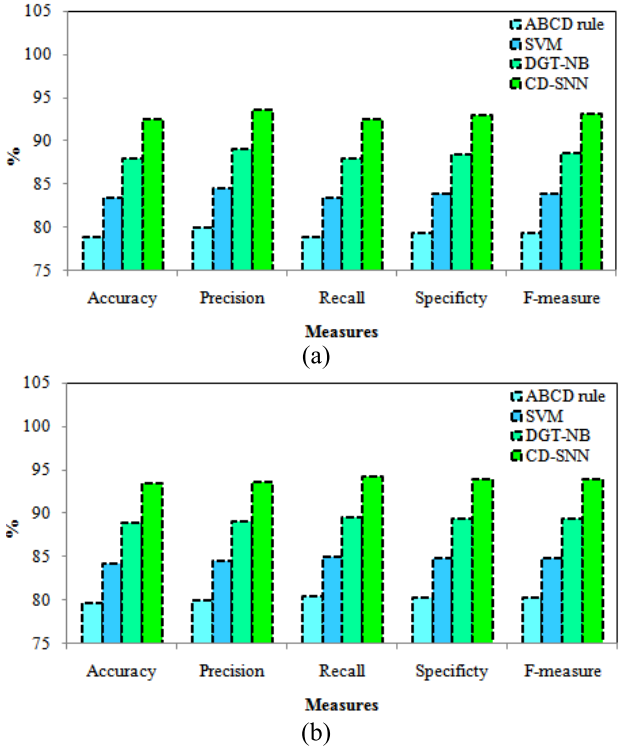

FIGURE 17. Results comparison of Carcinoma skin disease detection techniques for ISIC 2017 augmented dataset with (a) training case (b) testing case.

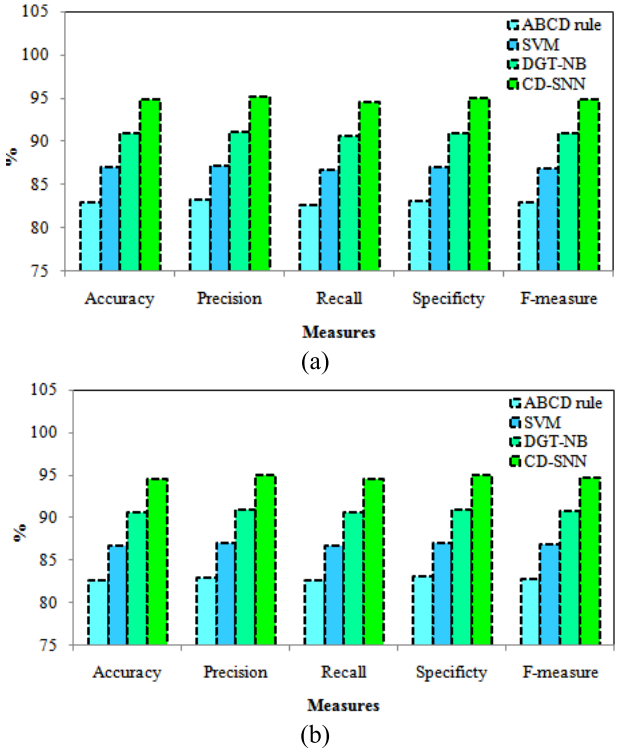

FIGURE 18. Results comparison of Blue Nevus skin disease detection techniques for ISIC 2017 augmented dataset with (a) training case (b) testing case.

comprising predictions and explanations, undergoes rigorous validation by domain specialists, typically dermatologists or skin disease experts. Their expertise ensures the reliability and accuracy of the model's predictions, validating the

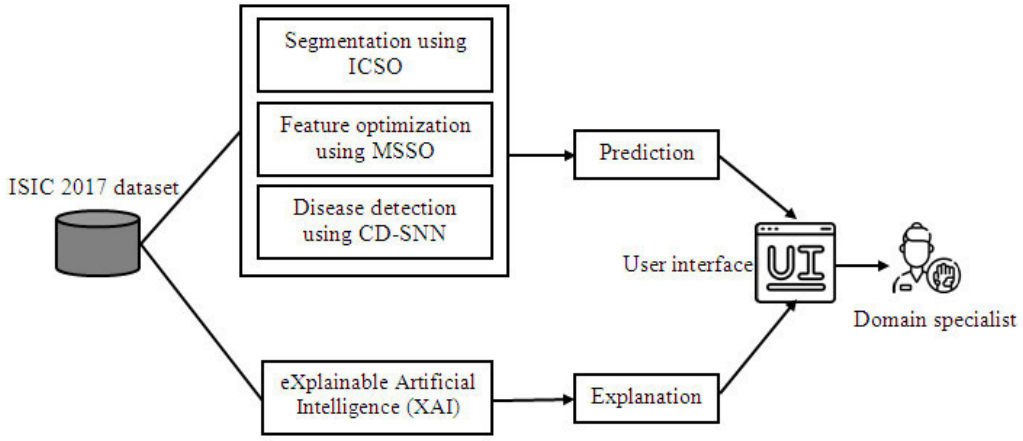

FIGURE 19. Interpretability of CD-SNN model using explainable artificial intelligence (XAI).

TABLE 6. Results of proposed CD-SNN technique for skin disease detection using commonly-used public datasets.

Dataset	Training				Testing			
	Accuracy	Precision	Recall	F-measure	Accuracy	Precision	Recall	F-measure
ISIC 2016	95.369	94.235	96.123	94.799	95.989	95.021	95.325	95.503
PH2	96.235	95.236	92.356	95.733	97.235	96.589	96.023	96.911
ISIC 2017 original	89.343	85.301	84.381	87.275	89.906	88.445	87.117	89.169
ISIC 2017 augmented	94.941	95.029	94.932	94.985	95.070	95.286	95.214	95.178

real-world applicability of our proposed framework. This comprehensive methodology not only improves prediction accuracy but also establishes a transparent and interpretable foundation for the CD-SNN model in skin disease detection.

E. GENERALIZABILITY OF PROPOSED MODEL

The assessment of the proposed CD-SNN technique extends beyond the primary focus on the ISIC2017 dataset, aiming to evaluate its generalizability across diverse datasets with variations in skin types, ethnicities, and disease manifestations. Table 6 provides a comparative analysis that offers valuable insights into the model's adaptability to different datasets. The evaluation on the ISIC 2016 dataset reveals the CD-SNN's nuanced understanding of diverse skin conditions. Despite sharing similarities with ISIC2017, the dataset presents distinct characteristics challenging the model's generalization. The marginal 0.62% improvement in testing accuracy indicates the model's ability to adapt to variations in disease manifestations within this dataset. The inclusion of the PH2 dataset, known for its unique skin conditions and ethnicities, serves as a robust test for the CD-SNN's generalizability. The notable 1.676% improvement in testing accuracy underscores the model's capacity to handle diverse skin types, emphasizing its potential application in broader demographic contexts. Within the ISIC 2017 dataset, both original and augmented, the CD-SNN exhibits consistent performance, highlighting its generalizability. The 0.917% improvement in testing accuracy for the original dataset and the marginal 0.129% decrease for the augmented dataset demonstrate the model's resilience and adaptability to diverse manifestations, even in the presence of augmented data complexities. In summary, the analysis across these datasets underscores the CD-SNN's robustness and adaptability to diverse skin conditions, ethnicities, and disease manifestations. These findings contribute to a comprehensive understanding of the model's potential applicability in real-world clinical scenarios, reinforcing its viability for dermatological diagnostics across diverse patient populations.

V. CONCLUSION

By combining effective segmentation and feature optimization with a hybrid deep learning technique, we present a methodology for the early identification and classification of skin disorders. The recently introduced ICSO algorithm optimizes segmentation, resulting in more precise identification of affected skin spots. The MSSO method has been used to address data dimensionality problems, which optimizes feature selection by determining the most significant and insightful features for classification. Furthermore, the CD-SNN has been introduced into the proposed method to improve the accuracy of skin disease detection and multiclass classification. The suggested method's performance is assessed using the benchmark ISIC 2017 dataset, which serves as a reliable benchmark for skin disease detection. According to the simulation results, our proposed CD-SNN technique achieved maximum detection accuracy in both

training and testing cases, with 93.235% and 95.070%, respectively. Moreover, from Table 5, we conclude that our proposed CD-SNN technique performs very effectively in the case of skin disease detection and classification, which achieves an average accuracy of 95.070% for the testing scenario. Clinical validation of DermCDSM's performance in real healthcare settings is crucial for its adoption. Overcoming the gap between research results and practical clinical application is a significant challenge that requires collaboration with medical professionals and regulatory approval. Moreover, the lack of interpretability may limit the acceptance of the model in clinical settings, where understanding the rationale behind predictions is crucial.

DECLARATION OF INTEREST

The authors declare that they have no conflict of interest.

ACKNOWLEDGMENT

The authors extend their appreciation to the Deputyship for Research & Innovation, Ministry of Education in Saudi Arabia for funding this research work through the project number ISP23-78.

REFERENCES

[1] K. Cluff, R. Becker, B. Jayakumar, K. Han, E. Condon, K. Dudley, G. Szatkowski, I. I. Pipinos, R. Z. Amick, and J. Patterson, "Passive wearable skin patch sensor measures limb hemodynamics based on electromagnetic resonance," *IEEE Trans. Biomed. Eng.*, vol. 65, no. 4, pp. 847–856, Apr. 2018, doi: 10.1109/TBME.2017.2723001.

[2] Y. Xia, L. Zhang, L. Meng, Y. Yan, L. Nie, and X. Li, "Exploring web images to enhance skin disease analysis under a computer vision framework," *IEEE Trans. Cybern.*, vol. 48, no. 11, pp. 3080–3091, Nov. 2018, doi: 10.1109/TCYB.2017.2765665.

[3] J. Zhang, Y. Xie, Y. Xia, and C. Shen, "Attention residual learning for skin lesion classification," *IEEE Trans. Med. Imag.*, vol. 38, no. 9, pp. 2092–2103, Sep. 2019, doi: 10.1109/TMI.2019.2893944.

[4] Z. Wu, S. Zhao, Y. Peng, X. He, X. Zhao, K. Huang, X. Wu, W. Fan, F. Li, M. Chen, J. Li, W. Huang, X. Chen, and Y. Li, "Studies on different CNN algorithms for face skin disease classification based on clinical images," *IEEE Access*, vol. 7, pp. 66505–66511, 2019, doi: 10.1109/ACCESS.2019.2918221.

[5] J. Yang, X. Wu, J. Liang, X. Sun, M.-M. Cheng, P. L. Rosin, and L. Wang, "Self-paced balance learning for clinical skin disease recognition," *IEEE Trans. Neural Netw. Learn. Syst.*, vol. 31, no. 8, pp. 2832–2846, Aug. 2020, doi: 10.1109/TNNLS.2019.2917524.

[6] Y. Gu, Z. Ge, C. P. Bonnington, and J. Zhou, "Progressive transfer learning and adversarial domain adaptation for cross-domain skin disease classification," *IEEE J. Biomed. Health Informat.*, vol. 24, no. 5, pp. 1379–1393, May 2020, doi: 10.1109/JBHI.2019.2942429.

[7] X. Fan, M. Dai, C. Liu, F. Wu, X. Yan, Y. Feng, Y. Feng, and B. Su, "Effect of image noise on the classification of skin lesions using deep convolutional neural networks," *Tsinghua Sci. Technol.*, vol. 25, no. 3, pp. 425–434, Jun. 2020, doi: 10.26599/TST.2019.9010029.

[8] K. Dietze, T. Moritz, T. Alexandrov, K. Krstevski, K. Schlottau, M. Milovanovic, D. Hoffmann, and B. Hoffmann, "Suitability of group-level oral fluid sampling in ruminant populations for lumpy skin disease virus detection," *Veterinary Microbiology*, vol. 221, pp. 44–48, Jul. 2018, doi: 10.1016/j.vetmic.2018.05.022.

[9] P. M. Burlina, N. J. Joshi, E. Ng, S. D. Billings, A. W. Rebman, and J. N. Aucott, "Automated detection of erythema migrans and other confounding skin lesions via deep learning," *Comput. Biol. Med.*, vol. 105, pp. 151–156, Feb. 2019, doi: 10.1016/j.compbiomed.2018.12.007.

[10] T. Y. Tan, L. Zhang, S. C. Neoh, and C. P. Lim, "Intelligent skin cancer detection using enhanced particle swarm optimization," *Knowledge-Based Syst.*, vol. 158, pp. 118–135, Oct. 2018, doi: 10.1016/j.knosys.2018.05.042.

[11] S. Chatterjee, D. Dey, and S. Munshi, "Integration of morphological preprocessing and fractal based feature extraction with recursive feature elimination for skin lesion types classification," *Comput. Methods Programs Biomed.*, vol. 178, pp. 201–218, Sep. 2019, doi: 10.1016/j.cmpb.2019.06.018.

[12] A. K. Verma, S. Pal, and S. Kumar, "Comparison of skin disease prediction by feature selection using ensemble data mining techniques," *Informat. Med. Unlocked*, vol. 16, Jun. 2019, Art. no. 100202, doi: 10.1016/j.imu.2019.100202.

[13] V. Horigan, P. M. Beard, H. Roberts, A. Adkin, P. Gale, C. A. Batten, and L. Kelly, "Assessing the probability of introduction and transmission of lumpy skin disease virus within the United Kingdom," *Microbial Risk Anal.*, vol. 9, pp. 1–10, Aug. 2018, doi: 10.1016/j.mran.2018.05.001.

[14] P. Shao, P. Yong, W. Zhou, J. Sun, Y. Wang, Q. Tang, S. Ren, Z. Wu, C. Zhao, Y. Xu, and X. Wang, "First isolation of photobacterium damselae subsp. Damselae from half-smooth tongue sole suffering from skin-ulceration disease," *Aquaculture*, vol. 511, Sep. 2019, Art. no. 734208, doi: 10.1016/j.aquaculture.2019.734208.

[15] S. Pathan, K. Gopalakrishna Prabhu, and P. C. Siddalingaswamy, "Automated detection of melanocytes related pigmented skin lesions: A clinical framework," *Biomed. Signal Process. Control*, vol. 51, pp. 59–72, May 2019, doi: 10.1016/j.bspc.2019.02.013.

[16] S. Serte and H. Demirel, "Gabor wavelet-based deep learning for skin lesion classification," *Comput. Biol. Med.*, vol. 113, Oct. 2019, Art. no. 103423, doi: 10.1016/j.compbiomed.2019.103423.

[17] S. Chatterjee, D. Dey, S. Munshi, and S. Gorai, "Extraction of features from cross correlation in space and frequency domains for classification of skin lesions," *Biomed. Signal Process. Control*, vol. 53, Aug. 2019, Art. no. 101581, doi: 10.1016/j.bspc.2019.101581.

[18] J. Möller, T. Moritz, K. Schlottau, K. Krstevski, D. Hoffmann, M. Beer, and B. Hoffmann, "Experimental lumpy skin disease virus infection of cattle: Comparison of a field strain and a vaccine strain," *Arch. Virology*, vol. 164, no. 12, pp. 2931–2941, Sep. 2019, doi: 10.1007/s00705-019-04411-w.

[19] T. Sreelatha, M. V. Subramanyam, and M. N. G. Prasad, "Early detection of skin cancer using melanoma segmentation technique," *J. Med. Syst.*, vol. 43, May 2019, Art. no. 190, doi: 10.1007/s10916-019-1334-1.

[20] D. A. Gavrilov, A. V. Melerzanov, N. N. Shchelkunov, and E. I. Zakirov, "Use of neural network-based deep learning techniques for the diagnostics (don't short) of skin diseases," *Biomed. Eng.*, vol. 52, no. 5, pp. 348–352, Jan. 2019, doi: 10.1007/s10527-019-09845-9.

[21] M. Chen, P. Zhou, D. Wu, L. Hu, M. M. Hassan, and A. Alamri, "AI-skin: Skin disease recognition based on self-learning and wide data collection through a closed-loop framework," *Inf. Fusion*, vol. 54, pp. 1–9, Feb. 2020, doi: 10.1016/j.inffus.2019.06.005.

[22] J. Bu, Y. Lin, L.-Q. Qing, G. Hu, P. Jiang, H.-F. Hu, and E.-X. Shen, "Prediction of skin disease using a new cytological taxonomy based on cytology and pathology with deep residual learning method," *Sci. Rep.*, vol. 11, Jul. 2021, Art. no. 13764, doi: 10.1038/s41598-021-92848-y.

[23] M. M. Mijwil, "Skin cancer disease images classification using deep learning solutions," *Multimedia Tools Appl.*, vol. 80, pp. 26255–26271, Apr. 2021, doi: 10.1007/s11042-021-10952-7.

[24] M. A. Khan, T. Akram, Y.-D. Zhang, and M. Sharif, "Attributes based skin lesion detection and recognition: A mask RCNN and transfer learning-based deep learning framework," *Pattern Recognit. Lett.*, vol. 143, pp. 58–66, Mar. 2021, doi: 10.1016/j.patrec.2020.12.015.

[25] E. Goceri, "Diagnosis of skin diseases in the era of deep learning and mobile technology," *Comput. Biol. Med.*, vol. 134, Jul. 2021, Art. no. 104458, doi: 10.1016/j.compbiomed.2021.104458.

[26] H. Q. Yu and S. Reiff-Marganiec, "Targeted ensemble machine classification approach for supporting IoT enabled skin disease detection," *IEEE Access*, vol. 9, pp. 50244–50252, 2021, doi: 10.1109/ACCESS.2021.3069024.

[27] P. N. Srinivasu, J. G. Sivasai, M. F. Ijaz, A. K. Bhoi, W. Kim, and J. J. Kang, "Classification of skin disease using deep learning neural networks with MobileNet v2 and LSTM," *Sensors*, vol. 21, no. 8, p. 2852, Apr. 2021, doi: 10.3390/s21082852.

[28] M. A. Khan, K. Muhammad, M. Sharif, T. Akram, and V. H. C. D. Albuquerque, "Multi-class skin lesion detection and classification via teledermatology," *IEEE J. Biomed. Health Informat.*, vol. 25, no. 12, pp. 4267–4275, Dec. 2021, doi: 10.1109/JBHI.2021.3067789.

[29] T. D. Nigat, T. M. Sitote, and B. M. Gedefaw, "Fungal skin disease classification using the convolutional neural network," *J. Healthcare Eng.*, vol. 2023, pp. 1–9, May 2023, doi: 10.1155/2023/6370416.

[30] V. R. Balaji, S. T. Suganthi, R. Rajadevi, V. K. Kumar, B. S. Balaji, and S. Pandiyan, "Skin disease detection and segmentation using dynamic graph cut algorithm and classification through naive Bayes classifier," *Measurement*, vol. 163, Oct. 2020, Art. no. 107922, doi: 10.1016/j.measurement.2020.107922.

[31] M. Kuffer, K. Pfeffer, R. Sliuzas, and I. Baud, "Extraction of slum areas from VHR imagery using GLCM variance," *IEEE J. Sel. Topics Appl. Earth Observ. Remote Sens.*, vol. 9, no. 5, pp. 1830–1840, May 2016, doi: 10.1109/JSTARS.2016.2538563.

[32] S. Aygün and E. O. Günes, "A benchmarking: Feature extraction and classification of agricultural textures using LBP, GLCM, RBO, neural networks, k-NN, and random forest," in *Proc. 6th Int. Conf. Agro-Geoinformatics*, Aug. 2017, pp. 1–4, doi: 10.1109/Agro-Geoinformatics.2017.8047000.

[33] F. Alamdar and M. Keyvanpour, "A new color feature extraction method based on QuadHistogram," *Proc. Environ. Sci.*, vol. 10, pp. 777–783, 2011, doi: 10.1016/j.proenv.2011.09.126.

[34] F. Tahir and M. A. Fahiem, "A statistical-textural-features based approach for classification of solid drugs using surface microscopic images," *Comput. Math. Methods Med.*, vol. 2014, pp. 1–12, 2014, doi: 10.1155/2014/791246.

[35] G. Loy and J.-O. Eklundh, "Detecting symmetry and symmetric constellations of features," in *Proc. Comput. Vis. ECCV*, 2006, pp. 508–521, doi: 10.1007/11744047_39.

[36] U. K. Lilhore, M. Poongodi, A. Kaur, S. Simaiya, A. D. Algarni, H. Elmannai, V. Vijayakumar, G. B. Tunze, and M. Hamdi, "Hybrid model for detection of cervical cancer using causal analysis and machine learning techniques," *Comput. Math. Methods Med.*, vol. 2022, pp. 1–17, May 2022, doi: 10.1155/2022/4688327.

[37] R. Tr, U. K. Lilhore, S. Simaiya, A. Kaur, and M. Hamdi, "Predictive analysis of heart diseases with machine learning approaches," *Malaysian J. Comput. Sci.*, pp. 132–148, Mar. 2022, doi: 10.22452/mjcs.sp2022no1.10.

[38] M. Abd Elaziz, A. Dahou, A. Mabrouk, S. El-Sappagh, and A. O. Aseeri, "An efficient artificial rabbits optimization based on mutation strategy for skin cancer prediction," *Comput. Biol. Med.*, vol. 163, Sep. 2023, Art. no. 107154.

[39] W. N. Ismail and H. A. Alsalamah, "Efficient Harris hawk optimization (HHO)-based framework for accurate skin cancer prediction," *Mathematics*, vol. 11, no. 16, p. 3601, Aug. 2023.

RUCHI MITTAL is currently a professional with over two decades of work experience in teaching, training, research, and academic administration. Her teaching expertise comprises DBMS, machine learning, social networking analysis, and data mining. She has published more than forty papers in Scopus/SCI-indexed journals, book series, and conference proceedings. She received the Chitkara University Research Excellence Award in author with the highest H-index category in 2020 (Computer Applications Discipline). She serves on the TPC of a number of conferences and is an Active Ph.D. Advisor. She reviews for a number of leading international journals, such as *Internet Research* (Emerald), *World Review of Science, Technology and Sustainable Development* (Inderscience), *International Journal of Computational Science and Engineering* (Inderscience), *International Journal of Intelligent Systems Technologies and Applications* (Inderscience), and a number of IEEE and Springer conferences.

FATHE JERIBI received the M.S. degree in computer science and information technology from Sacred Heart University, Fairfield, CT, USA, and the Ph.D. degree in information technology from Towson University, Towson, MD, USA. He is currently an Associate Professor with the College of Computer Science and Information Technology, Jazan University, Saudi Arabia. His areas of research interests include machine learning, software engineering, computer networks, SDN, wireless ad hoc networks, the IoT, and distributed computing. He serves as a reviewer for peer-reviewed journals.

R. JOHN MARTIN received the Ph.D. degree in computer science from Bharathiar University, India, with a focus on an innovative machine-learning model for epileptic seizure detection using EEG signals. He is currently a Distinguished Educator in computer science and holds expertise in machine learning, healthcare AI, and signal processing, spanning a 27-year career in higher education, research, and educational leadership. He is also teaching with Jazan University, Saudi Arabia. His impactful works feature in the prestigious journals of IEEE and ACM. Notably, he holds international patents and copyrights, showcasing ground-breaking healthcare AI innovations.

VARUN MALIK (Member, IEEE) received the Ph.D. degree in computer science and engineering from I. K. Gujral Punjab Technical University, Punjab, India. He is currently holding more than ten Indian patents/copyrights. His current research interests include blockchain, artificial intelligence, cloud computing, cyber security, the Internet of Things, data mining and warehousing, and method engineering. He serves as a reviewer for many international journals.

SANTHOSH JOSEPH MENACHERY received the M.D. degree in medical pharmacology from Manipal University (MAHE), India. He is currently an Assistant Professor with the Department of Clinical Pharmacy. He has published extensively in PubMed-indexed journals in the areas of clinical pharmacology. He has excellent academic experience and also has experience with competitive intelligence in pipeline drugs.

JAITEG SINGH received the Ph.D. degree in computer science and engineering. He has more than 17 years of experience in research, development, and teaching with the Institutes of Higher Technical Education. His research interests include software engineering, business intelligence, data and opinion mining, cartography, curriculum design, pedagogical innovation, neuro marketing, educational technology, offline navigation systems, and cloud computing.